A Squid Dynein Isoform Promotes Axoplasmic Vesicle Translocation

Susan P. Gilbert*§ and Roger D. Sloboda‡§

*Department of Molecular and Cell Biology, Pennsylvania State University, University Park, PA 16802; ‡Department of Biological Sciences, Dartmouth College, Hanover, New Hampshire 03755; and §The Marine Biological Laboratory, Woods Hole, Massachusetts 02543

Abstract. Axoplasmic vesicles that translocate on isolated microtubules in an ATP-dependent manner have an associated ATP-binding polypeptide with a previously estimated relative molecular mass of 292 kD (Gilbert, S. P., and R. D. Sloboda. 1986. *J. Cell Biol.* 103:947–956). Here, data are presented showing that this polypeptide (designated Hl) and another high molecular mass polypeptide (H2) can be isolated in association with axoplasmic vesicles or optic lobe microtubules. The Hl and H2 polypeptides dissociate from microtubules in the presence of MgATP and can be further purified by gel filtration chromatography. The peak fraction thus obtained demonstrates MgATPase activity and promotes the translocation of salt-extracted vesicles (mean = 0.87 μm/s) and latex beads (mean = 0.92 μm/s) along isolated microtubules. The Hl polypeptide binds [α^{32}P]8-azidoATP and is thermosoluble, but the H2 polypeptide does not share these characteristics. In immunofluorescence experiments with dissociated squid axoplasm, affinity-purified Hl antibodies yield a punctate pattern that corresponds to vesicle-like particles, and these antibodies inhibit the bidirectional movement of axoplasmic vesicles. H2 is cleaved by UV irradiation in the presence of MgATP and vanadate to yield vanadate-induced peptides of 240 and 195 kD, yet Hl does not cleave under identical conditions. These experiments also demonstrate that the actual relative molecular mass of the Hl and H2 polypeptides is ~435 kD. On sucrose density gradients, Hl and H2 sediment at 19–20 *S*, and negatively stained samples reveal particles comprised of two globular heads with stems that contact each other and extend to a common base. The results demonstrate that the complex purified is a vesicle-associated ATPase whose characteristics indicate that it is a squid isoform of dynein. Furthermore, the data suggest that this vesicle-associated dynein promotes membranous organelle motility during fast axoplasmic transport.

DIRECTED intracellular organelle movement occurs in association with cytoplasmic microtubules in many types of eukaryotic cells. Initially, the requirement for microtubules was inferred from both morphological observations and from physiological studies in which the depolymerization of microtubules by pharmacological agents was accompanied by the cessation of organelle translocations. More recently, with the application of video microscopy techniques to microtubule-dependent motility, it was possible to observe directly single microtubules and the movement of individual particles along them. Moreover, these methods permitted the development of in vitro model systems to define and characterize the organelle–cytoskeletal interactions that occur to promote translocation and to confer specificity for the direction of particle movement (for review see 24, 57, 61, 71).

The observation of Lasek and Brady (39) that the nonhydrolyzable analogue of ATP, adenylyl imidodiphosphate, promoted the attachment of squid axoplasmic organelles to microtubules to form a stable complex led to the discovery and characterization of kinesin, a new mechanochemical force transducer (7, 64, 72). Since these first studies, kinesin has been purified from many different cells and tissues and shown to be a ubiquitous force-generating protein. It mediates the plus end–directed translocation of latex beads along microtubules and microtubule gliding on glass coverslips at a rate of ~0.5 μm/s and contains a major polypeptide with relative molecular mass of 110–130 kD and one or more light chains of ~40–80 kD (for reviews see 71, 79, 80).

Because axoplasmic microtubules are oriented with their plus ends distal to the cell body (8, 27), kinesin is thought to be the mechanochemical enzyme that propels organelles toward the terminal region during orthograde transport. When antibodies to the 110-kD polypeptide of squid kinesin were used to remove kinesin from an axoplasmic supernatant (73), the resulting supernatant stimulated bead movement from the plus to minus ends of microtubules: i.e., the direction opposite to that promoted by kinesin. Furthermore, the minus end–directed bead movement demonstrated pharmacological properties characteristic of axonemal dynein—inhibition by 20 μM vanadate and inhibition by *N*-ethylmaleimide. These in vitro motility experiments suggested that there are two distinct mechanochemical enzymes responsible for fast axoplasmic transport: kinesin for orthograde or-

ganelle movement and another, possibly dynein-like protein, for retrograde transport.

To identify putative cytoplasmic dyneins, investigators have characterized high molecular mass polypeptides that copurify with microtubules and compared the properties of these microtubule-associated proteins (MAPs) with those of flagellar and ciliary dyneins (13, 21, 29, 31, 42, 47, 49, 52, 55, 81). This strategy has permitted the identification of dynein isoforms in diverse species and tissues, including MAP 1C from bovine brain (48, 49, 76), the nematode *Caenorhabditis elegans* translocator (42), HMWP from the freshwater amoeba *Reticulomyxa*, and the rat Sertoli cell MAP, designated HMW-2 (47). In contrast to the other microtubule-dependent translocators purified, the *Reticulomyxa* protein promoted bidirectional movement of latex beads. Porter et al. (52) characterized two distinct isoforms of dynein in unfertilized sea urchin eggs. One form appeared more closely related to axonemal dynein, and the authors suggested that it may be a ciliary precursor. The other dynein isoform, previously designated HMr-3 (63), demonstrated characteristics in common with putative organelle translocators.

The approach that we have taken to determine the molecular mechanism of force generation during fast axonal transport is to identify the ATP-binding polypeptides of axoplasmic vesicles that translocate on isolated microtubules and to evaluate these nucleotide-binding proteins as candidates for mechanochemical enzymes (20–22). The use of the photoaffinity analogue of ATP, [α^{32}P]8-azidoadenosine 5′-triphosphate ([α^{32}P]8-azidoATP), directed our attention to a high molecular mass polypeptide (designated here as Hl and referred to previously as 292 kD [21] or vesikin [12, 66]; see Results) that bound the ATP analogue. The experiments presented here examine the characteristics of the Hl polypeptide as a microtubule-based organelle translocator and show that this polypeptide and another high molecular mass MAP (H2) are subunits of a 19–20-*S* protein complex. The complex has ATPase activity and promotes the translocation along microtubules of both latex beads and salt-extracted axoplasmic vesicles. Immunofluorescence studies localize the Hl polypeptide to the surface of what appear by differential interference contrast (DIC) video-enhanced microscopy to be membranous axoplasmic organelles, and affinity-purified Hl antibodies inhibit axoplasmic vesicle motility in dissociated axoplasm. Lastly, UV-induced vanadate-sensitive photocleavage experiments and an examination of the 19–20-*S* particles by electron microscopy reveal that this organelle translocator is a squid isoform of dynein.

Materials and Methods

Materials

Squid *Loligo pealei* were obtained from the Department of Marine Resources (Marine Biological Laboratory, Woods Hole, MA). Mouse monoclonal antibodies to α-tubulin were purchased from Miles Scientific Div. (Naperville, IL); CNBr-activated Sepharose 4B was from Pharmacia Fine Chemicals (Piscataway, NJ); and carboxylated latex beads (0.15 μm diameter, 2.5% solid/solution) were from Polysciences, Inc. (Warrington, PA). Bio-gel A-1.5m (200–400 mesh), gel filtration standards, electrophoresis purity acrylamide, *N,N′*-methylene-bisacrylamide, and urea were obtained from Bio-Rad Laboratories (Richmond, CA). [α^{32}P]8-azidoATP was purchased at a specific activity of 11–13 Ci/mmole from ICN Radiochemicals (Irvine, CA). [γ^{32}P]ATP was obtained at a specific activity of 3,000 Ci/mmole from New England Nuclear (Boston, MA) or ICN Radiochemicals. All other biochemicals were purchased from Sigma Chemical Co. (St. Louis, MO).

1. *Abbreviations used in this paper*: DIC, differential interference contrast; MAP, microtubule-associated protein.

Protein and Vesicle Purification

Hl/H2. Hl/H2 was prepared either from freshly dissected squid optic lobes or from optic lobes that had been frozen in liquid N_2 and stored at −80°C until use. Optic lobes were homogenized at 4°C in a volume of PM buffer (100 mM Pipes, pH 6.9, 10 mM $MgSO_4$, 10 mM EGTA, 1 mM PMSF, 20 μg/ml leupeptin, 1 mM DTT, 0.5 mM GTP) that was 1.5 times the wet weight of the optic lobes. The homogenate was centrifuged at 31,000 *g* for 30 min at 4°C. The supernatant was removed and clarified by centrifugation (180,000 *g* for 90 min at 4°C). The supernatant was removed, adjusted to 1 mM GTP and 20 μM taxol, and incubated at 4°C for 45 min to polymerize the microtubules. The microtubules were collected by centrifugation (39,100 *g* for 30 min at 4°C) and resuspended in PM-taxol buffer (PM buffer plus 20 μM taxol). The microtubules were sedimented by centrifugation over a 10% sucrose cushion in PM-taxol buffer. The resulting washed microtubule pellets were resuspended in PM-taxol buffer, adjusted to 10 mM MgATP, and incubated for 15 min at 26°C. The preparation was centrifuged at 39,100 *g* for 30 min at 4°C. The supernatant (referred to here as the first ATP release) was removed and stored on ice. The microtubule pellets were resuspended in PM-taxol buffer and adjusted to 10 mM MgATP as before. After incubation at 26°C for 15 min, the preparation was centrifuged as described above. The supernatant (the second ATP release) was removed, combined with the first ATP release, and concentrated.

The concentrated ATP-released fraction was clarified by centrifugation (180,000 *g* for 40 min at 4°C). The supernatant was removed and applied to a Bio-Gel A-1.5m column (1.5 cm × 40 cm) that was equilibrated in 20 mM Hepes, pH 7.2, 50 mM KCl, 5 mM $MgSO_4$, 1 mM EGTA, 10 μg/ml leupeptin, 1 mM DTT, 0.1 mM MgATP. Approximately ninety 0.73-ml fractions were collected. The peak fractions containing Hl/H2 polypeptides as determined by gel electrophoresis were pooled and dialyzed overnight against 20 mM Hepes, pH 7.2, 50 mM KCl, 5 mM $MgSO_4$, 1 mM EGTA, 1 mM DTT, 2 mM PMSF. The dialysate was then clarified by centrifugation and concentrated for ~2 h using microconcentrators (Centricon 30; Amicon Corp., Danvers, MA) to a final protein concentration of ~1–3 mg/ml. This preparation was stored on ice until use.

For some experiments, the ATP-released fraction was dialyzed against the Hepes buffer, concentrated, and clarified for analysis by sucrose density gradient centrifugation by the method of Martin and Ames (44). Samples (0.5–1 ml) were applied to 5–25% sucrose gradients (11.5 ml) and centrifuged at 33,000 rpm for 16 h in a rotor (SW41; Beckman Instruments, Inc., Palo Alto, CA). Eighteen 0.6-ml fractions were then collected from the top of each tube by the application of 40% sucrose to the bottom of the tube. The gradient fractions were analyzed by gel electrophoresis and tested for ATPase activity as discussed below.

Routinely, the purification began with 70 g of optic lobes which yielded ~7–8 mg of protein as the combined ATP-released supernatant. After gel filtration chromatography, dialysis, concentration, and clarification of the preparation, ~1 ml of protein at 0.9–1.8 mg/ml resulted. The sucrose gradient purification of the 19–20-*S* fraction of Hl/H2 yielded ~0.2–0.3 mg of protein at 0.03–0.05 mg/ml.

The thermosoluble preparation of Hl was prepared by adjusting squid microtubules in PM-taxol buffer to 0.75 M NaCl and 1 mM DTT. The microtubule solution was transferred to a boiling water bath for 5 min and then cooled rapidly. After centrifugation, the supernatant containing heat soluble Hl was removed, dialyzed, concentrated, and stored on ice until use.

Axoplasmic Vesicles. Vesicles were isolated from extruded axoplasm (5–8 μl/axon) obtained from 12–14 giant axons of the squid *L. pealei* using discontinuous sucrose gradient centrifugation as previously described (20). The vesicles from the sucrose gradient were extracted with 2 M potassium acetate to remove peripheral membrane proteins. The vesicles and solubilized peripheral membrane proteins were then separated by Sephacryl S-400 column chromatography performed at room temperature in a plastic disposable 5-ml pipette containing 4 ml of resin equilibrated in 20 mM Hepes, pH 7.2, 50 mM KCl, 5 mM $MgSO_4$, 1 mM EGTA, 20 μg/ml leupeptin, 1 mM DTT. Fractions of 200 μl were collected, and protein was determined using a spot assay (3) and SDS-PAGE (see below). The fractions containing vesicles free of soluble proteins were pooled and concentrated using microconcentrators (Centricon-30; Amicon Corp.).

Mammalian Brain Tubulin. Porcine brain microtubules were prepared by two cycles of temperature-dependent polymerization and depolymerization (65, 67), and tubulin was separated from microtubule-associated poly-

peptides by the method of Borisy et al. (5). For the in vitro motility assays, the tubulin was thawed and assembled at 22°C with 20 μM taxol plus 0.1 mM GTP. The assembled microtubules were then diluted in the Hepes buffer plus 20 μM taxol.

Biochemical Assays

ATPase Assays. ATPase activity was determined in Hepes buffer (20 mM Hepes, pH 7.2, 50 mM KCl, 5 mM $MgSO_4$, 1 mM EGTA) at 22°C and pH 7.2. A coupled assay system was used in which phosphoenolpyruvate and pyruvate kinase constitute the ATP-regenerating component of the assay, while the loss of NADH catalyzed by lactate dehydrogenase provides the optical signal needed to monitor the coupled reaction. The final concentrations within the cuvette were 0.2 mM NADH, 1 mM phosphoenolpyruvate, 10 U/ml pyruvate kinase, 5 U/ml lactate dehydrogenase, Hl/H2 protein (0–0.6 mg/ml), and MgATP (0–2 mM). The disappearance of NADH as a measure of ATP hydrolysis was monitored as the decrease in absorbance at 340 nm. Control experiments demonstrated that the regeneration of ATP by pyruvate kinase was not limited by the conditions used. To assay for ATPase activity in the sucrose gradient fractions, the formation of $^{32}P_i$ from [γ^{32}P]ATP was determined as described previously (34).

Photoaffinity Labeling. Hl/H2 preparations were labeled radioactively with [α^{32}P]8-azidoATP (ICN Radiochemicals) as previously described (21). The 100-μl aliquots contained a final concentration of 0.2 mg/ml protein and 10 μM [α^{32}P]8-azidoATP (specific activity of 11–13 Ci/mmole).

Vanadate-sensitive UV Cleavage. The supernatant that resulted from extraction of optic lobe microtubules with 10 mM MgATP was clarified by centrifugation. This supernatant enriched in Hl and the resuspended microtubule pellet enriched in H2 were adjusted to 100 μM vanadate from a stock solution of 100 mM sodium orthovandate. Because commercial preparations of sodium orthovandate contain varying amounts of water, the concentration of the stock solution of vanadate was established by the procedure of Vogel (78) which uses vanadium pentoxide (V_2O_5) as a standard. The Hl and H2 samples were irradiated on ice for varying times (0–360 min) with 366-nm light (19, 37, 40). Aliquots were then reduced and analyzed by SDS-PAGE.

Protein Determination. Protein concentration was determined by the Schacterle and Pollack (59) modification of the procedure of Lowry et al. (41). For preparations that contained DTT, protein concentrations were determined by the method of Bradford (6).

Preparation and Characterization of Hl Antibodies

Antiserum against Hl was produced in New Zealand white rabbits using the following procedures. After electrophoresis, the band corresponding to Hl was excised from the gel and incubated in PBS until the pH of the solution stabilized at 7. A quantity of the gel equal to ~100 μg of protein was combined with a similar volume of PBS; this sample was then homogenized in an equal volume of Freund's complete adjuvant, and the rabbit was injected subcutaneously with this mixture. An identical subcutaneous booster injection (this time with incomplete adjuvant) was given after 4 wk. 1 wk after the boost, the serum tested positive for Hl antibodies by immunoblotting. The rabbit was boosted again 2 wk later and bled for serum 2 wk after the second boost. The boosting and bleeding schedule was repeated. The IgG fraction was obtained from the preimmune and immune sera by precipitation with ammonium sulfate at 50% saturation, followed by resuspension of the pellet in and dialysis against PBS.

Antibodies to Hl were further purified using affinity column chromatography with purified Hl (see Fig. 1, lane *c*) bound to CNBr-activated Sepharose 4B using the procedure supplied by the manufacturer (Pharmacia Fine Chemicals). The affinity-purified Hl antibodies were eluted from the column by the addition of 2 ml of 0.2 M glycine-HCl, pH 2.8, immediately brought to ~pH 6 by the addition of 2 ml of 10× PBS, and then dialyzed against PBS to remove the glycine and bring the antibodies to pH 7. The affinity-purified antibodies were then concentrated at 4°C for use in Western blotting, motility, and immunofluorescence experiments (see below).

Electrophoretic transfer of proteins from polyacrylamide gels to nitrocellulose paper (0.2 μm) was performed according to the method of Towbin et al. (70). After the transfer was completed, the nitrocellulose sheets were processed for detection of rabbit IgG-antigen immune complexes by the use of alkaline phosphatase–conjugated secondary antibodies (4).

SDS-PAGE

Protein samples were analyzed using 4–10% acrylamide, 2–8 M urea linear gradient; or 5% acrylamide, 2 M urea; or 3% acrylamide, 8 M urea slab gels (0.75 mm) with 3% stacking gels according to the buffer formulations of Laemmli (38) and stained for protein with Coomassie brilliant blue R 250 (15) or silver nitrate (45, 56). In silver stains, Hl stains bright orange to yellow, depending upon protein concentration, and H2 stains jet black.

Light and Electron Microscopy

Video-enhanced DIC and Fluorescence Microscopy. Preparations were observed by video-enhanced DIC microscopy (1, 32) as described previously (21). For observation of the slides prepared for double label immunofluorescence (see below), the microscope was used with epifluorescence illumination, and the fluorescent image was projected onto the silicon-intensified target of a camera (C-1000-12; Hamamatsu Corp., Middlesex, NJ) that was coupled to an image processor (C1966; Photonic Microscopy, Inc., Oak Brook, IL) for frame averaging to increase the signal-to-noise ratio. Images were recorded in real time. For reproduction of images from the videotapes, micrographs were photographed directly from the video monitor (using a 50-line Ronchi diffraction grating placed in front of the camera lens) onto 35-mm Plus-X film (Eastman Kodak Co., Rochester, NY) that was developed in Microdox-X (Eastman Kodak Co.).

Indirect Immunofluorescence. Samples for immunofluorescence were processed by previously published procedures (62). The coverslips were mounted with *p*-phenylenediamine in buffered glycerol (33) and observed as described in the preceding section.

Motility Experiments

Hl Antibody Inhibition. For the experiments in which the effect of affinity-purified Hl antibodies on motility was evaluated, the antibodies as well as various control preparations (see text and Table I) were dialyzed against motility buffer (20 mM Hepes, pH 7.2, 175 mM potassium aspartate, 65 mM taurine, 85 mM betaine, 25 mM glycine, 6.4 mM $MgCl_2$, 2 mM EGTA, 2 mM PMSF, 20 μg/ml leupeptin, 2 mM MgATP) and then concentrated to obtain a protein concentration of ~4 mg/ml. Axoplasm from three squid giant axons was extruded, added to 50 μl of motility buffer, incubated at 4°C for 15 min, and homogenized by pipetting 50 times using a Gilson P200 Pipetman (Rainin Instrument Co. Inc., Woburn, MA). The preparations of axoplasm consistently yielded a protein concentration of 7–8 mg/ml. 3 μl of the axoplasmic preparation were combined with 3 μl of test sample (see text), and then 5 μl were added to a coverslip (No. 0; 24 × 50 mm), covered by a second coverslip (No. 0; 18 × 18 mm), sealed with vaseline/lanolin/paraffin (1:1:1), and transferred to the microscope for observation by video-enhanced DIC microscopy as described above. Routinely, a given microscope field of a preparation was observed for 10–15 min, and a minimum of three fields per preparation was evaluated during a 30–45-min time period. Each test sample (buffer, BSA, preimmune antibodies, Tu27B, and Hl affinity-purified antibodies) was examined using at least four different axoplasmic preparations. A single homogenized axoplasmic preparation was used for no longer than 3 h, and, during this time period, no difference in motility in control experiments was observed.

Hl/H2 Promoted Motility. The ability of gel filtration–purified Hl/H2 to support motility was assessed using three types of assays: (*a*) Hl/H2 promoted microtubule gliding on glass; (*b*) Hl/H2 promoted movement of salt-extracted axoplasmic vesicles on microtubules; and (*c*) Hl/H2 promoted movement of latex beads on microtubules. For the different assays, the microtubules were assembled from purified porcine brain tubulin with 0.1 mM GTP plus 20 μM taxol. An aliquot of 3 μl Hl/H2 (0–0.5 mg/ml) was added to 1–3 μl of microtubules (0.1 mg/ml), salt-extracted axoplasmic vesicles, or carboxylated latex beads (2.5% solid solution diluted 50-fold in Hl/H2 buffer). The buffer conditions were as follows: 20 mM Hepes, pH 7.2, 50–100 mM KCl, 5 mM $MgSO_4$, 1 mM EGTA, 20 μM taxol, 0–2 mM MgATP. Each preparation was added to a coverslip as described above and then transferred to the microscope for observation by video-enhanced DIC microscopy. A given microscope field of a preparation was observed for 10–30 min, and a minimum of five fields per preparation was evaluated. The data in Fig. 4 *A* (vesicle motility) represent three separate preparations of salt-extracted axoplasmic vesicles and three separate preparations of gel filtration–purified Hl/H2. The data in Fig. 4 *B* (bead motility) represent four separate preparations of Hl/H2. The preparations used for the vesicle motility experiments were also used for the bead motility experiments. The rates of vesicle and bead movement were determined from video records of motility along straight segments of microtubules. The distance of translocation was determined by calculating the distance measured on the video monitor from the beginning to end of the translocation. The time was calculated from the time display on the video monitor at the beginning and end of the translocation. Statistical analysis of motility data used *t* test and the Mann-Whitney *U* test.

Electron Microscopy. For transmission electron microscopy, the gel filtration preparations and the 12–13-*S* and 19–20-*S* sucrose gradient fractions were negatively stained on carbon films according to the method of Valentine et al. (75).

Results

Previously, we observed that axoplasmic vesicles isolated in the presence of MgATP retained the ability to translocate on axonemal microtubules (22); and photoaffinity experiments using the radioactive analogue of ATP, [α^{32}P]8-azidoATP, identified a high molecular mass polypeptide (referred to here as Hl) that remained associated with these vesicles during purification (21). However, when taxol-assembled microtubules were isolated from squid optic lobes in the absence of MgATP but in the presence of GTP, Hl sedimented with the microtubules (Fig. 1, lane *b*; Fig. 5 in reference 21). In addition, another high molecular mass polypeptide, H2, also sedimented with the optic lobe microtubules. Because Hl and H2 purified with microtubules and Hl cross reacted with a polyclonal antiserum to porcine brain MAP 2 (21), the squid Hl and H2 polypeptides were compared with mammalian brain MAPs. The optic lobe microtubules (Fig. 1, lane *b*) were adjusted to 0.75 M NaCl plus 1 mM DTT and boiled for 5 min. Under these conditions mammalian brain MAP 1 precipitates, but MAP 2 remains soluble (16, 28, 36). The heat treatment of optic lobe microtubules (Fig. 1, lane *b*) yielded a supernatant (lane *c*) that contained Hl only, demonstrating the thermosolubility of Hl and not H2. Thus, Hl is similar to vertebrate brain MAP 2 with respect to heat stability.

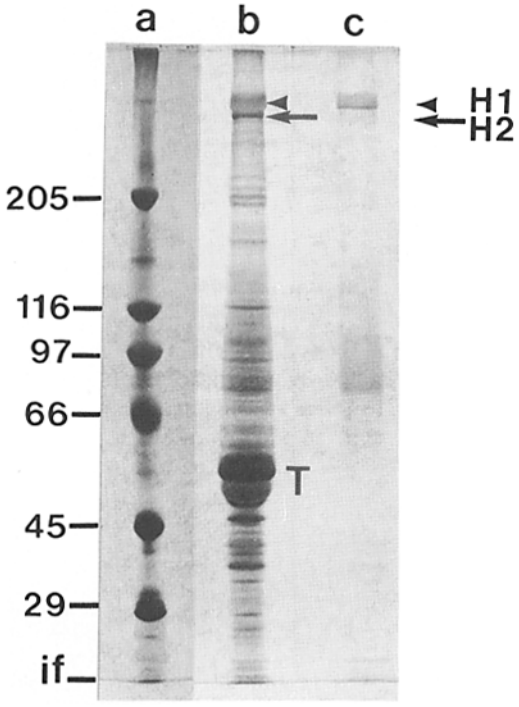

Figure 1. Cosedimentation of Hl and H2 polypeptides with squid optic lobe microtubules. Optic lobe microtubules were purified by taxol assembly, and lane *b* shows the cosedimentation of the Hl and H2 polypeptides with tubulin (*T*). This preparation of optic lobe microtubules was then heat treated as described in Materials and Methods to compare Hl and H2 with mammalian brain MAPs. Lane *c* shows the supernatant that results and demonstrates that Hl is thermosoluble, yet H2 is not. The gel lanes are from a single 5–10% acrylamide, 2–8 M urea gradient slab gel stained with silver nitrate: (lane *a*) molecular mass standards (in kilodaltons); (lane *b*) the microtubules before heating; (lane *c*) thermosoluble Hl. (*Arrowhead*) Hl; (*arrow*) H2; *T*, α- and β-tubulin; *if*, ion front.

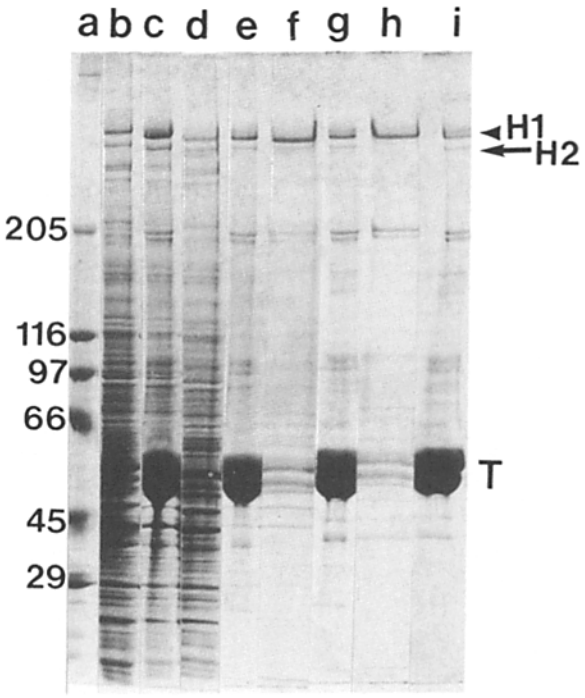

Figure 2. MgATP-dependent release of Hl and H2 from optic lobe microtubules. Taxol-assembled optic lobe microtubules were purified in the absence of ATP but in the presence of GTP, washed with buffer, and then extracted with 10 mM MgATP. This series of Coomassie blue–stained gel lanes is from a single 4–10% acrylamide, 2–8 M urea slab gel. (Lane *a*) Molecular mass markers in kilodaltons; (lane *b*) 50 K supernatant; (lane *c*) microtubules polymerized in the presence of taxol; (lane *d*) supernatant above the washed microtubules; (lane *e*) washed microtubules; (lane *f*) supernatant of the first MgATP release; (lane *g*) resulting microtubules of first release; (lane *h*) supernatant of the second MgATP release; (lane *i*) resulting microtubules of second release. *T*, α- and β-tubulin.

Purification, Motility, and ATPase Activity of Hl/H2

Fig. 2 shows the purification of Hl and H2 with taxol-assembled optic lobe microtubules (lane *e*) isolated in the absence of ATP and shows the ATP-dependent release of these polypeptides to the supernatant when the microtubules were extracted with 10 mM MgATP (lanes *f* and *h*). Because GTP was included in the homogenization buffer and each subsequent step of the isolation, kinesin remained soluble and did not sediment with the microtubules and associated polypeptides. Furthermore, the dissociation of Hl and H2 from the microtubules required the addition of either MgATP or MgCTP, but MgGTP did not promote the specific release of Hl and H2 to the supernatant (data not shown). Hl and H2 were further purified from the ATP extracts by gel filtration column chromatography to yield three peaks of protein as shown in Fig. 3 *A*. The major peak of Hl/H2 was in the void volume (lane *c*), and the ATP-binding polypeptides of this

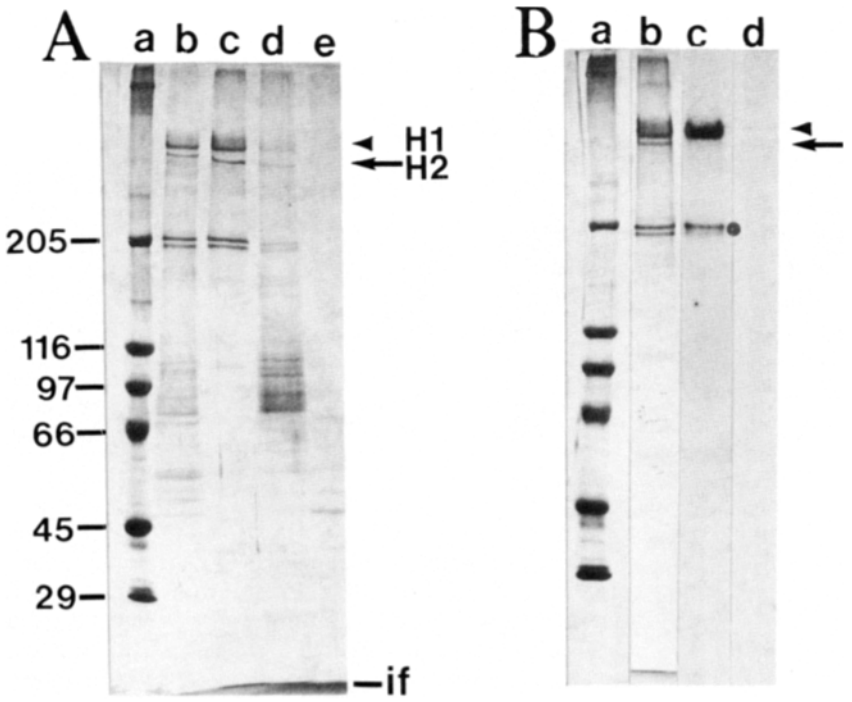

Figure 3. Purification of H1/H2 from the ATP-released supernatant by gel filtration. (*A*) Protein elutes from the Bio-Gel A-1.5m column in three peaks: the fractions from each peak were pooled, dialyzed, and concentrated, and a representative sample of each appears in the following gel lanes. Each lane is from a single 4–10% acrylamide, 2–8 M urea gradient slab gel that was silver stained: (lane *a*) molecular mass standards in kilodaltons; (lane *b*) concentrated, clarified ATP-released material (Fig. 2, lanes *f* and *h*) that was loaded onto the column; (lane *c*) protein composition of the peak fractions of H1 and H2 polypeptides, eluting at the void volume of the column; (lane *d*) protein composition of the first included peak; (lane *e*) protein composition of the second included peak. (*B*) The purified H1/H2 fraction (A, lane *c*) was covalently modified with [α^{32}P]8-azido-ATP to determine the ATP-binding polypeptides of the preparation: (lane *a*) molecular mass standards; (lane *b*) silver-stained gel of Bio-Gel A-1.5m purified H1/H2 plus [α^{32}P]8-azidoATP after UV irradiation. Lanes from the corresponding autoradiographs show the photoaffinity labeling of H1/H2 fraction with [α^{32}P]8-azidoATP in the presence (lane *c*) and the absence (lane *d*) of UV irradiation. (*Arrowhead*) H1; (*arrow*) H2; (•) proteolytic fragment of H1 (see text and Fig. 7); *if*, ion front.

fraction were determined by photoaffinity labeling using [α^{32}P]8-azidoATP (Fig. 3 *B*). Fig. 3 B, lane *c*, is from the autoradiograph and shows that in the presence of UV irradiation H1 bound the ATP analogue, yet H2 clearly did not. The doublet (•) at ~200 kD that incorporated label is believed to be a proteolytic fragment of H1 containing the ATP-binding domain because it cross reacts with affinity-purified H1 antibodies (see Fig. 7, lanes *i* and *j*).

The gel filtration peak fraction of H1/H2 (Fig. 3 *A*, lane *c*) in the presence of 1 mM MgATP promoted the motility of salt-extracted vesicles and carboxylated latex beads along taxol-stabilized, MAP-free porcine brain microtubules (Figs. 5 and 6). The isolated axoplasmic vesicles were incubated in 2 M potassium acetate to remove peripheral membrane proteins, and these salt-extracted vesicles were then separated from the soluble proteins by gel filtration chromatography (Fig. 4). The fractions enriched in vesicles but free of soluble proteins (Fig. 4, lane *b*) were concentrated, incubated with soluble H1/H2, and tested for the ability of H1/H2 to promote axoplasmic vesicle motility. Fig. 5 *A* shows the translocation of a salt-extracted axoplasmic vesicle at 1.04 μm/s for a distance of 2.8 μm. H1/H2 also promoted the motility of latex beads along isolated microtubules (Fig. 5 *B*), and the bead shown moved for a distance of 4.5 μm at a rate of 0.79 μm/s. Analysis of the videotapes revealed as many as one to three translocations per minute, but most vesicle and bead translocations were for short distances (≤1 μm). After a brief movement, the bead or vesicle would suddenly dissociate from or appear to fall off the microtubule. Those vesicles and beads that did move for longer distances (3–6 μm) frequently demonstrated translocations that contained very brief pauses or hesitations, and the longer translocations were less frequent—approximately three to five per 10-min observation. Control experiments demonstrated that beads and salt-extracted vesicles did not undergo directed movement in the absence of added H1/H2.

The characteristics of the salt-extracted vesicle motility were not visually different from those of the latex beads, and the mean rate of vesicle motility (0.87 μm/s) was not significantly different from the mean rate of latex bead motility (0.92 μm/s) at a $P \leq 0.05$ (Fig. 6). The translocations characterized by rates of 0.5 μm/s (Fig. 6) were of the longer translocations that contained hesitations or brief pauses. Mo-

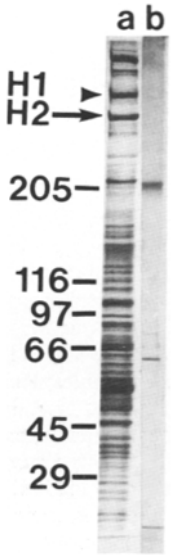

Figure 4. Polypeptide composition of salt-extracted axoplasmic vesicles. Isolated vesicles were extracted with 2 M potassium acetate to remove peripheral membrane proteins, and the vesicles were then purified by gel filtration chromatography to separate vesicles from soluble proteins. The samples were resolved on 4–10% acrylamide, 2–8 M urea gradient slab gels that were silver stained. (Lane *a*) The vesicles before the salt treatment; (lane *b*) the vesicles that result after the salt extraction and gel filtration column chromatography. Molecular mass markers (in kilodaltons) are indicated to the left of lane *a*.

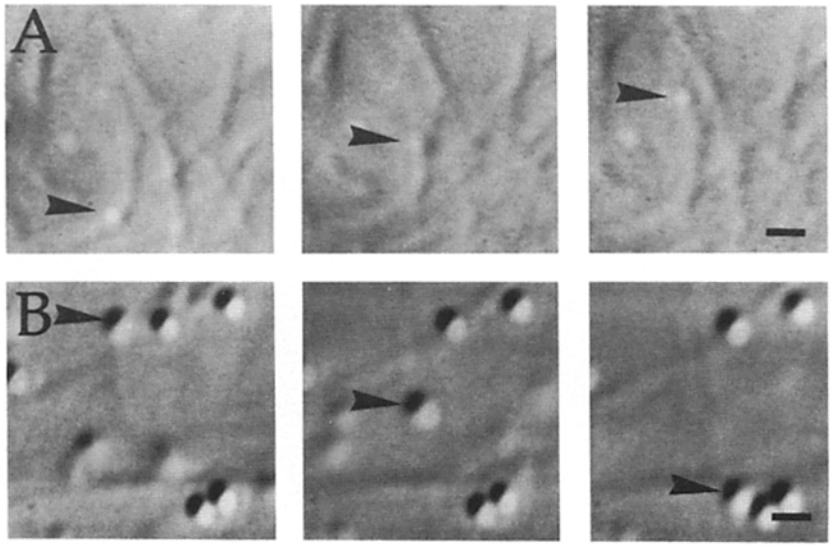

Figure 5. The translocation of salt-extracted axoplasmic vesicles and latex beads on isolated microtubules promoted by H1/H2 plus 1 mM MgATP. (*A*) The vesicle (*arrowhead*) moved for 2.8 μm at a rate of 1 μm/s along the taxol-stabilized MAP-free microtuble. (*B*) The 4.5-μm translocation of a latex bead (*arrowhead*) at a rate of 0.7 μm/s. Bars: (*A*) 0.8 μm; (*B*) 0.9 μm.

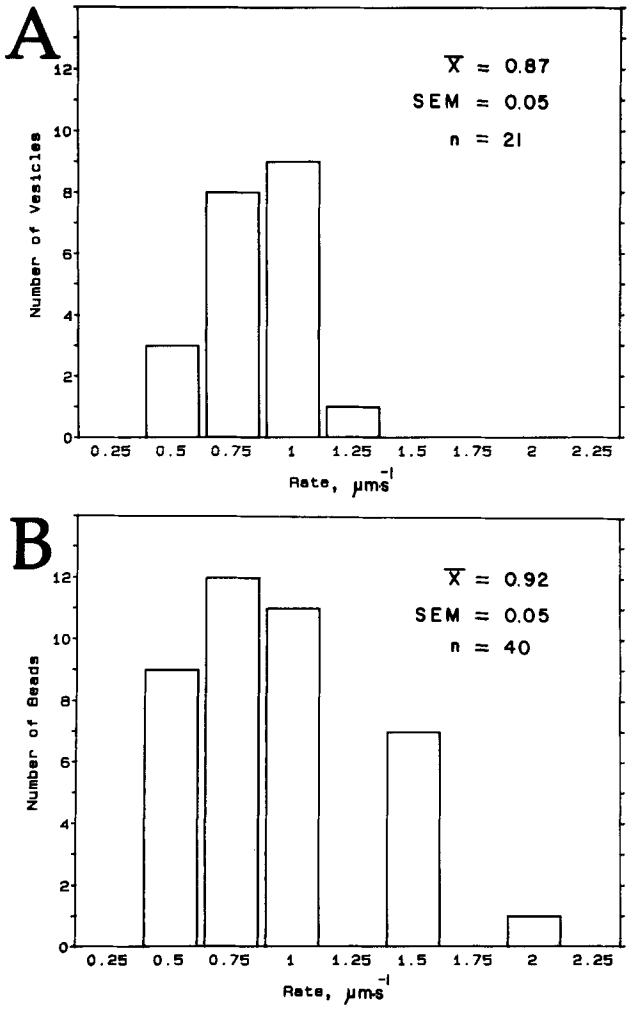

Figure 6. Rates of vesicle and bead movement on microtubules. The gel filtration-purified preparation of H1/H2 (Fig. 3 *A*, lane *c*) promoted the translocation of salt-extracted vesicles (*A*) and latex beads (*B*) along taxol-assembled MAP-free microtubules. The rates of 0.5 μm/s represent translocations that contained pauses and hesitations (see Materials and Methods and Results). The mean rate of vesicle movement was not significantly different from the mean rate of bead movement ($P \leq 0.05$). $\bar{X}$, mean.

tility of both salt-extracted vesicles and latex beads was promoted by fractions containing H1/H2, including the supernatant that resulted after extraction of the optic lobe microtubules with MgATP (Fig. 2, lane *f*, and Fig. 3 *A*, lane *b*) as well as the peak fraction of soluble H1/H2 after gel filtration chromatography (Fig. 3 *A*, lane *c*). Furthermore, all preparations that promoted the movement of salt-extracted vesicles also promoted the movement of latex beads, but microtubule gliding promoted by H1/H2 was not observed. As the soluble H1/H2 preparations aged, the number of translocations per unit time decreased. However, for those vesicles and beads that did move, the characteristics and the rates of vesicle and bead motility did not appear different from motility promoted by freshly purified H1/H2.

ATPase assays of the gel filtration preparations of H1/H2 (Fig. 3 *A*, lane *c*) demonstrate that the rate increases with increasing concentration of H1/H2 (0–0.6 mg/ml final concentration) as well as with increasing MgATP concentration (0–2 mM MgATP). These results indicate that H1/H2 demonstrates a soluble MgATPase activity according to Michaelis–Menten kinetics with a V_{max} = 0.015 μmol/mg per min and a K_m = 56 μM.

Immunofluorescence Using Affinity-purified H1 Antibodies

Rabbit polyclonal antibodies to H1 were affinity purified by column chromatography using the thermosoluble preparation of H1 (Fig. 1, lane *c*). Because H2 and the other high molecular mass polypeptides precipitated when the microtubules were boiled, the use of thermosoluble H1 for affinity purification ensured that no antibodies to H2 or other high molecular mass polypeptides would be present with the H1 antibodies.

Fig. 7 shows the characterization of the affinity-purified H1 antibodies. The H1 antibodies cross reacted with H1 in association with optic lobe microtubules (lanes *c* and *d*), with H1 present in the supernatant that results after the extraction of optic lobe microtubules with MgATP (lanes *e* and *f*), with H1 present in two preparations purified by gel filtration chromatography (lanes *g–j*). Lane *i* shows a doublet (•) that migrates near the heavy chain of rabbit skeletal myosin (lane

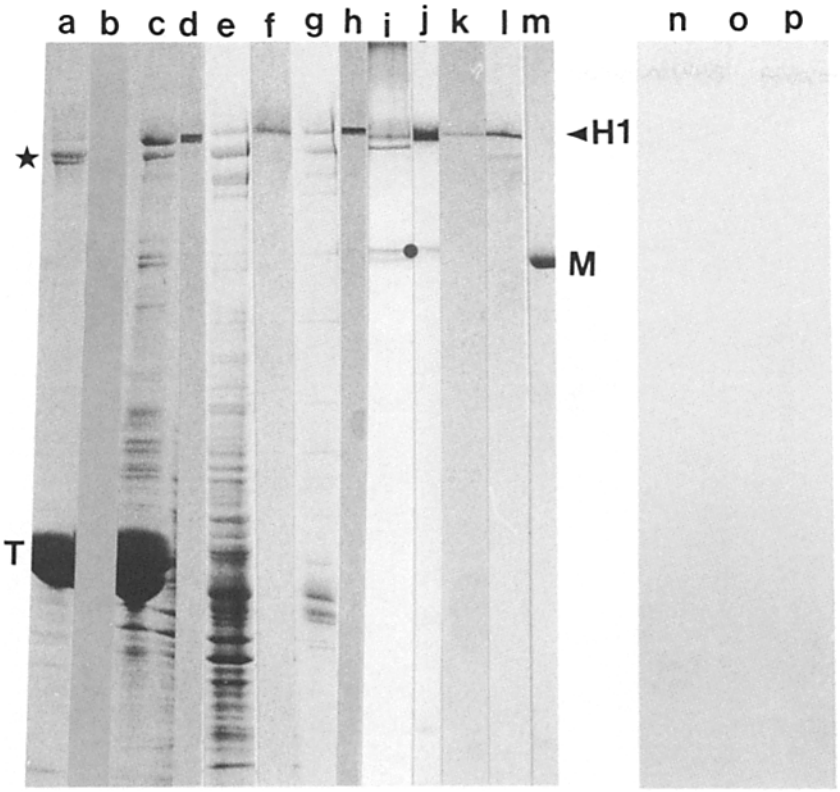

Figure 7. Immunoblot characterization of affinity-purified H1 antibodies. Rabbit polyclonal antibodies were prepared to gel slices of optic lobe H1, and the H1 antibodies were affinity purified using the thermosoluble preparation of H1 (Fig. 1, lane *c*). Samples were resolved on 4–10% acrylamide, 2–8 M urea gels, transferred to nitrocellulose, and probed with either affinity-purified H1 antibodies or with preimmune antibodies. (Lanes *a*, *c*, *e*, *g*, *i*, *k*, and *m*) Slab gels stained with silver nitrate; (lanes *b*, *d*, *f*, *h*, *j*, and *l*) blots probed with H1 antibodies at a dilution of 1:500; (lanes *n–p*) blots probed with preimmune antibodies at a dilution of 1:100. (Lanes *a*, *b*, and *n*) porcine brain microtubules; (lanes *c*, *d*, and *o*) optic lobe microtubules; (lanes *e* and *f*) MgATP extract of optic lobe microtubules; (lanes *g*, *h*, *i*, and *j*) two different gel filtration preparations of H1/H2; (lanes *k* and *l*) thermosoluble H1; (lane *m*) rabbit skeletal myosin; (lane *p*) low speed (16 K) optic lobe supernatant. (★) MAP 2; (*arrowhead*) H1; *T*, tubulin subunits; *M*, myosin heavy chain.

m), and this doublet shows cross-reaction with the affinity-purified H1 antibodies (lane *j*). Blots containing this gel filtration preparation of H1 were also probed with antibodies to the heavy chain of squid optic lobe myosin, and no cross reaction with the doublet polypeptides was evident (data not shown). The H1 antibodies recognized thermosoluble H1 (lanes *k* and *l*) and H1 from squid axoplasm (Fig. 8 *A*, lanes *c* and *d*). Although on some blots a weak cross-reaction with porcine brain MAP 2 (Fig. 7, lane *a*; ★) was evident, the level of reaction was considerably less than that demonstrated by H1, and most blots showed no cross-reaction with porcine brain MAPs (Fig. 7, lanes *a* and *b*). Preimmune antibodies showed no cross-reaction with porcine brain microtubules, optic lobe microtubules, a low speed optic lobe supernatant (Fig. 7, lanes *n–p*, respectively), or squid axoplasm (Fig. 8 *A*, lane *e*).

Previous experiments indicated that H1 was a component of isolated axoplasmic vesicles that translocate along microtubules (21). To demonstrate conclusively that H1 was associated with membranous organelles in axoplasm, double label immunofluorescence experiments were performed in squid axoplasm using the affinity-purified H1 antibodies (Fig. 8 *B*). Extruded axoplasm was incubated in a low ionic strength buffer and dispersed by pipetting to cause the microtubules to dissociate into single transport filaments. This dissociated axoplasmic preparation was previously shown to support bidirectional particle movements along single microtubules (2, 62, 74). Furthermore, this preparation was homogeneous, and the decreased viscosity of dissociated axoplasm ensured that the transport filaments were freely accessible to the antibodies.

Fig. 8 *B* shows the DIC and immunofluorescence micrographs of a single microscope field of a fixed preparation of dissociated axoplasm treated with mouse monoclonal antibodies to α-tubulin and affinity-purified H1 antibodies. Fig. 8 *B*, panel *a*, is of the DIC video micrograph with vesicle-like particles indicated by the white arrowheads and black arrows; panel *b* shows the corresponding epifluorescence micrograph generated with tubulin antibodies; and panel *c* shows the epifluorescence micrograph generated with H1 antibodies. Panel *b* illustrates the linear staining pattern of the axoplasmic microtubules. In contrast, the H1 fluorescence pattern (panel *c*) is punctate and corresponds to vesicle-like particles that are apparent in the DIC micrograph (panel *a*, *white arrowheads*). Although most of the vesicle-like particles cross reacted with H1 antibodies, not all the vesicle-like particles labeled; some that did not react with H1 antibodies are indicated by the black arrows (panel *a*). Conversely, some fluorescent signal identifying H1 (panel *c*) has no counterpart in the corresponding DIC image (panel *a*). Presumably, the frame averaged image from the sensitive silicon-intensified target camera can detect fluorescent particles not observed by video-enhanced DIC. The observation that the H1 staining pattern was punctate and not linear like that of tubulin suggests that H1 does not associate with the wall of the microtubule in a spatially periodic fashion as one would expect for a microtubule-associated protein as classically defined (11, 36, 46, 67). Rather, these results demonstrate that H1 is normally associated with vesicle-like particles in squid axoplasm.

H1 Antibody Inhibition of Axoplasmic Vesicle Motility

The affinity-purified antibodies to H1 were used in motility experiments with axoplasm to ascertain their effect on vesicle motility (Table I). Extruded axoplasm was diluted in the low ionic strength motility buffer described above to obtain a ho-

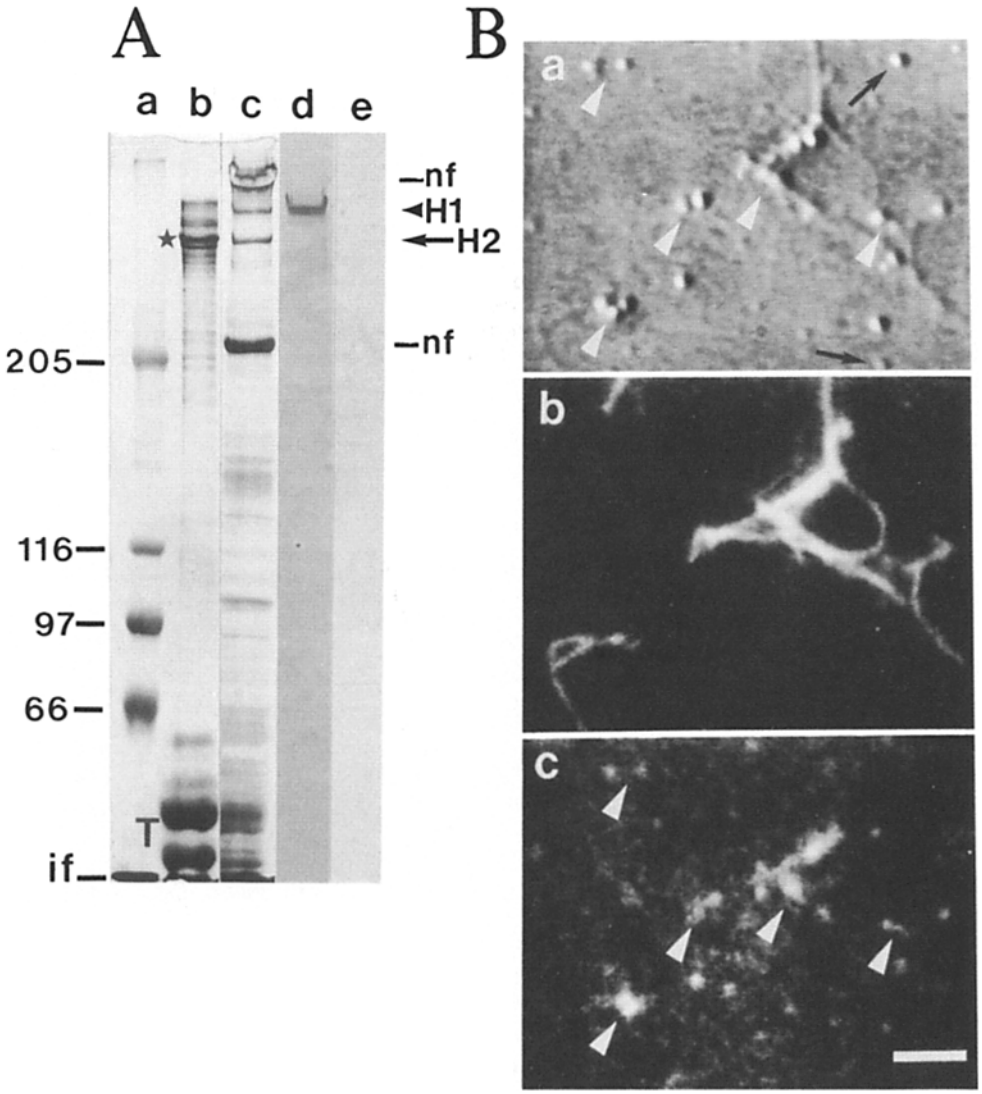

Figure 8. H1 antibody specificity and double label immunofluorescence of squid axoplasm. (*A*) Lanes *a–c* are from a silver-stained 5% acrylamide, 2 M urea gel: (lane *a*) molecular mass standards (in kilodaltons); (lane *b*) porcine brain microtubules; (lane *c*) squid axoplasm. Lanes *d* and *e* show immunoblots of the axoplasm challenged with affinity-purified H1 antibodies at 1:500 (lane *d*) and preimmune antibodies at 1:100 (lane *e*). The affinity-purified antibodies to optic lobe H1 react with axoplasmic H1. (★) MAP 2; *nf*, neurofilament polypeptides; *T*, tubulin subunits; *if*, ion front. (*B*) Dissociated squid axoplasm was treated simultaneously with affinity-purified H1 antibodies and monoclonal antibodies to α-tubulin. (Panel *a*) Video-enhanced DIC image of an area of fixed dissociated axoplasm showing a number of vesicle-like particles, many of which are in association with microtubules. The resolution of this DIC image is compromised somewhat due to the nonideal refractive index of the anti-bleach mounting medium used for immunofluorescence. (Panel *b*) Fluorescence micrograph of the same field as in panel *a*, generated here by fluorescein-labeled goat anti-mouse secondary antibodies, thus revealing the tubulin staining pattern. (Panel *c*) Fluorescence micrograph of the same field as in panels *a* and *b*, generated here by rhodamine-conjugated goat anti-rabbit secondary antibodies, thus revealing the subcellular distribution of H1. Note the punctate staining pattern in panel *c* as compared with the continuous staining pattern of the microtubules in panel *b*. Not all vesicle-like particles react with H1 antibodies. The white arrowheads point to vesicle-like particles visible in DIC that react with H1 antibodies while the black arrows point to particles visible in DIC that do not react with these antibodies. Bar, 427 nm.

mogeneous preparation of single transport filaments that supported bidirectional motility. Various antibodies as well as BSA used as a control were dialyzed against this motility buffer and concentrated to approximately the same concentration before use. The data in Table I show that affinity-purified H1 antibodies inhibited axoplasmic vesicle movement in a concentration-dependent manner. Interestingly, H1 antibodies inhibited motility in both directions on microtubules to the same extent, such that maximally effective concentrations of H1 antibodies blocked all vesicle movements in the in vitro–dissociated axoplasmic motility system. However, preimmune antibodies, monoclonal antibodies to β-tubulin, and BSA at similar concentrations showed no discernable effect on vesicle motility.

The results presented thus far suggested to us that we had purified an organelle translocator. Our next series of experiments was directed to determine if this translocator was unique or rather a squid isoform of dynein.

Vanadate-sensitive UV Photocleavage of H2

The role of H2 in promoting vesicle and bead motility was not clear because H2 was not observed to bind [α^{32}P]8-azidoATP as expected for a dynein heavy chain, yet it purified with H1 during gel filtration chromatography. When $MgCl_2$ was substituted for $MgSO_4$ in the optic lobe microtubule buffer, H1 could be purified away from H2. Fig. 9, lane *b*, shows the supernatant obtained by centrifugation after extraction of optic lobe microtubules with 10 mM MgATP, and this supernatant was greatly enriched for H1. The microtubule pellet that results (lane *h*) was enriched for H2, but some H1 was present also.

These two preparations were irradiated at 366 nm in the presence of MgATP and sodium orthovanadate to determine if either polypeptide showed the vanadate-specific UV photocleavage characteristic of axonemal dyneins (19, 37, 40). The data in Fig. 9 indicate that irradiation of the H1-enriched supernatant did not generate cleavage peptides (lanes *b–g*).

Table I. Inhibition of Organelle Movement by Affinity-purified H1 Antibodies

3 μl diluted axoplasm (7–8 mg/ml)	Movement
+ 1 μl anti-H1 + 2 μl buffer	+++ to ++
+ 2 μl anti-H1 + 1 μl buffer	+
+ 3 μl anti-H1 (3.8 mg/ml)	−
+ 3 μl preimmune antibodies (3.9 mg/ml)	++++
+ 3 μl buffer	++++
+ 3 μl Tu27B (4 mg/ml)	++++
+ 3 μl BSA (3 mg/ml)	++++

For each test sample (H1 antibodies, preimmune antibodies, Tu27B, BSA, and buffer) noted, four to eight different dissociated axoplasmic preparations were observed (see Materials and Methods). Each microscope coverslip preparation was evaluated for 30–45 min, and a minimum of three fields was observed for 10–15 min each. The resulting motility was scored on a scale of no motility during the time of observation −) to some motility (at least two organelles moving during the time of observation [+]) to normal motility (++++).

However, H2 did demonstrate photocleavage to generate peptides with relative molecular masses of 240 and 195 kD (lanes *h–l*), and the photocleavage was induced by vanadate because in the absence of vanadate, the 240- and 195-kD peptides were not generated (lane *m*). The vanadate-sensitized UV photocleavage of H2 but not H1 was somewhat unexpected because the [α^{32}P]8-azidoATP-binding experiments indicated that H2 was not an ATP-binding polypeptide. In fact, the [α^{32}P]8-azidoATP binding data and the vanadate-specific UV cleavage results originally indicated to us that H1 was not a dynein but rather a unique organelle-associated polypeptide. Therefore, in some abstracts as well as two symposium papers, H1 was referred to as vesikin to indicate its vesicle association (12, 66). However, an alternative interpretation of the [α^{32}P]8-azidoATP data is that at the time of labeling, H2 already had nucleotide tightly bound at its ATP-binding site even after overnight dialysis. Lastly, the UV vanadate-sensitive cleavage of H2 to generate peptides of 240 and 195 kD indicates that the true native subunit of H2 has a relative molecular mass of ~435 kD, and therefore the actual relative molecular mass of H1 is somewhat greater than this value.

Sedimentation Analysis of H1 and H2 Polypeptides

The supernatant that resulted after extraction of optic lobe microtubules with MgATP was dialyzed, concentrated, and then centrifuged on 5–25% sucrose gradients. The 18 frac-

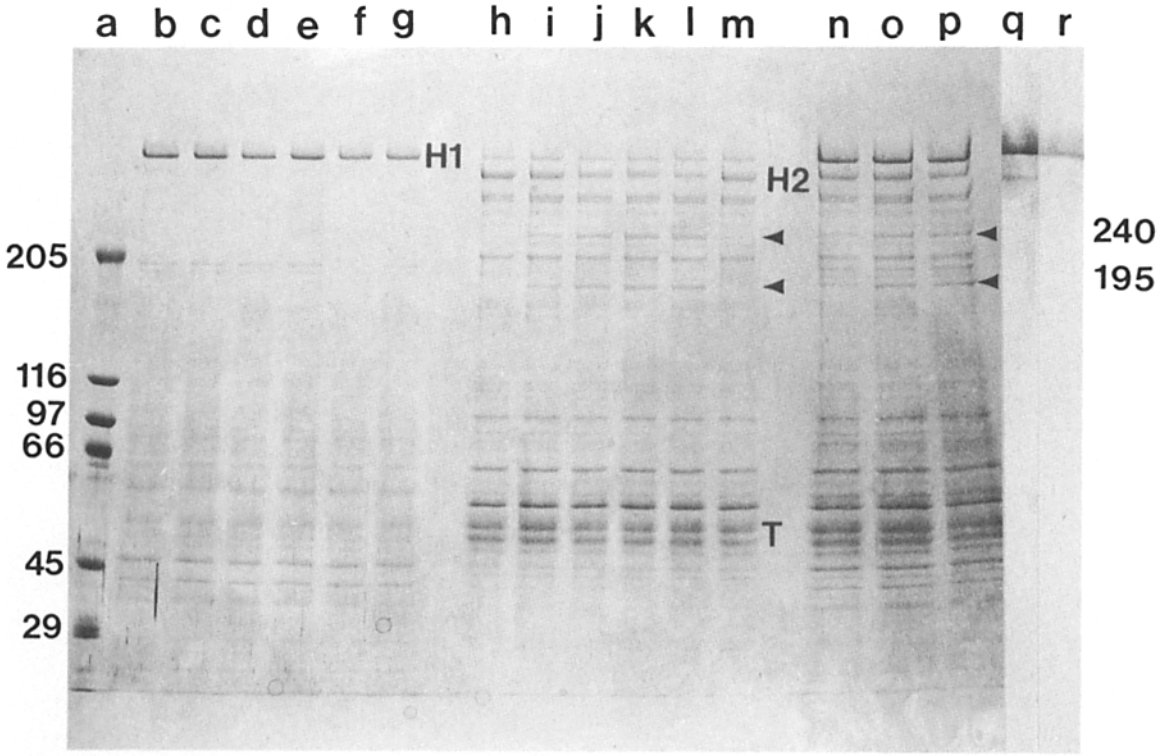

Figure 9. Vanadate-induced UV photocleavage of H2. H1 was purified away from H2 by substitution of $MgCl_2$ for $MgSO_4$ in the buffer. The supernatant that results after extraction of microtubules with 10 mM MgATP was enriched in H1 (lane *b*). The microtubule pellet that results (lane *h*) contained some H1 but was enriched for H2. These two preparations were exposed to 366-nm light in the presence of 100 μM vanadate plus 10 mM MgATP, and the samples were analyzed by SDS-PAGE on 4–10% acrylamide, 2–8 M urea gels stained with Coomassie blue. Lanes *b–f* show irradiation of the H1-enriched supernatant for 0, 30, 60, 90, and 120 min, respectively, in the presence of MgATP and vanadate. Lane *g* shows irradiation for 120 min in the presence of MgATP but absence of vanadate. No cleavage peptides were evident in the presence or absence of vanadate. The microtubule pellet (enriched for H2) was resuspended in buffer, MgATP, and vanadate and irradiated for 0, 30, 60, 90, and 120 min (lanes *h–l*, respectively). There was a progressive decrease in H2 and a progressive increase in cleavage peptides (*arrowheads*) at 240 and 195 kD. In the absence of vanadate (lane *m*), no cleavage peptides were evident. Lanes *n–p* show irradiation of the combined supernatant and microtubule pellet in the presence of vanadate and MgATP for 30, 60, and 90 min (lanes *n–p*, respectively). Immunoblots of the H1 (lane *q*) and H2 (lane *r*) samples (lanes *f* and *g*, respectively) were probed with affinity-purified H1 antibodies, and no cross-reaction with cleavage peptides at 240 and 195 kD was evident in either sample.

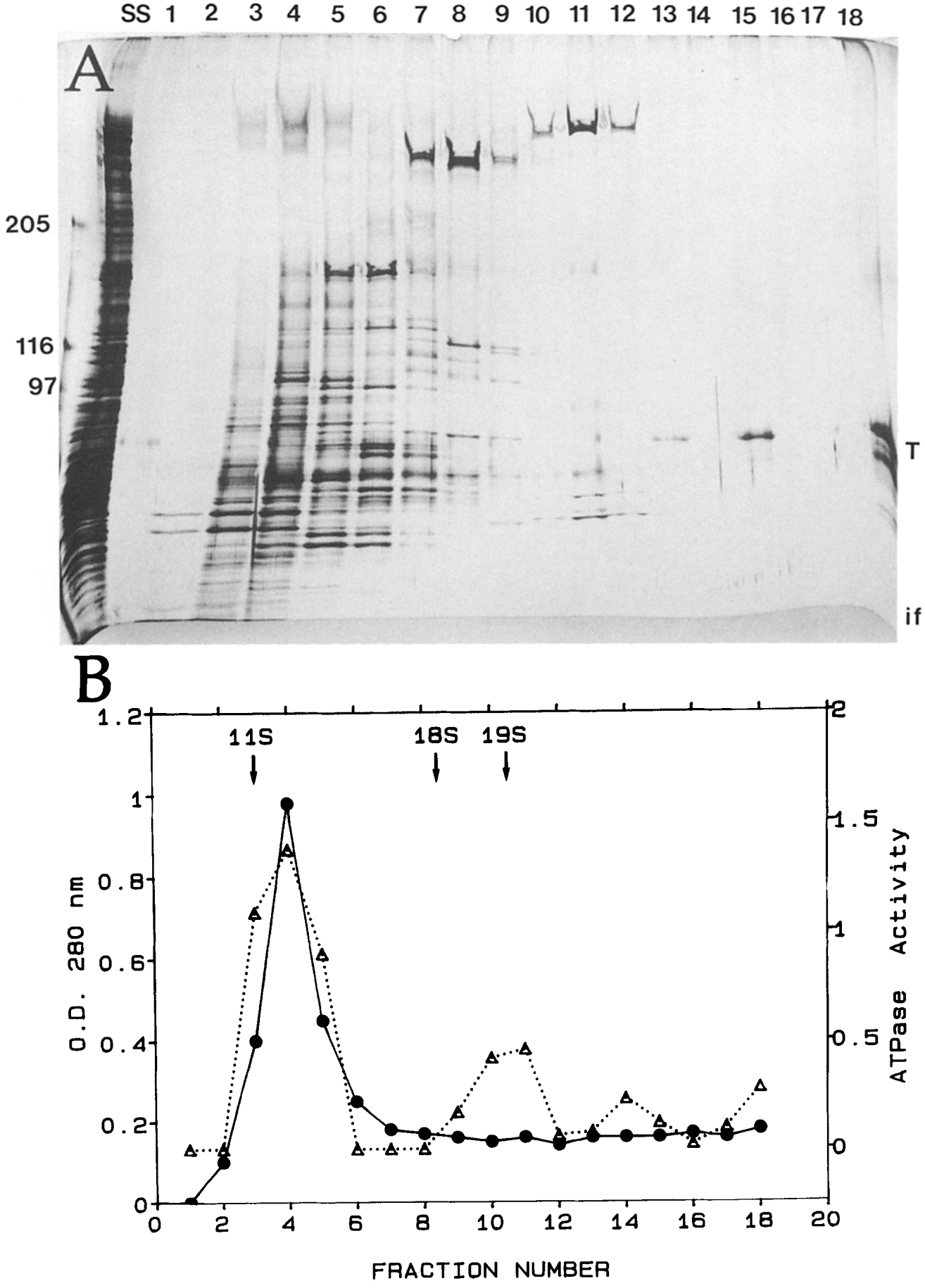
SS 1 2 3 4 5 6 7 8 9 10 11 12 13 14 15 16 17 18
A
205
116
97
T
if
B
11S
18S
19S
1.2
1
0.8
0.6
0.4
0.2
0
O.D. 280 nm
2
1.5
1
0.5
0
ATPase Activity
0 2 4 6 8 10 12 14 16 18 20
FRACTION NUMBER

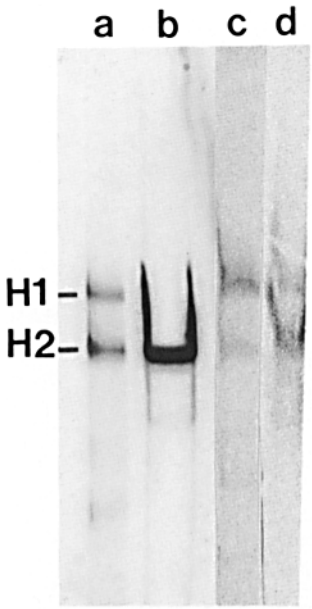

Figure 11. Polypeptide composition of 12–13-*S* and 19–20-*S* sucrose gradient fractions. Lanes *a* and *b* are from the top of a silver-stained 3% acrylamide, 8 M urea gel and lanes *c* and *d* are from the corresponding Western blot probed with affinity-purified H1 antibodies. Lane *a* is of the 12–13-*S* fraction, and two polypeptides are evident. Both stained bright orange (see Materials and Methods), and the corresponding Western blot (lane *c*) demonstrates that both polypeptides cross reacted with the H1 antibodies. These data indicate the presence of two species of H1. Lane *b* shows the 19–20-*S* fraction. One gel band was evident at the H2 region, but it stained both black and orange. The immunoblot (lane *d*) shows the cross-reaction with the H1 antibodies, thus indicating the sedimentation of the H1 polypeptide as well as H2 at 19–20 *S*.

tions were assayed for ATPase activity and analyzed by SDS-PAGE (Fig. 10). Two peaks of ATPase activity at 12–13 *S* and 19–20 *S* (Fig. 10 *B*, fractions *3–5* and *10–11*) correspond to fractions containing H1 and H2 polypeptides (Fig. 10 *A*). Fig. 11 shows the 12–13-*S* and 19–20-*S* peak fractions resolved on a 3% acrylamide, 8 M urea silver-stained gel and the corresponding Western blot probed with affinity-purified H1 antibodies. The H1 and H2 polypeptides were observed to stain differently on silver-stained gels (see Materials and Methods); H1 always stained yellow to orange, and H2 always stained intense black. Fig. 11, lane *a*, shows the gel of the 12–13-*S* fraction. Both polypeptides stained orange, and the corresponding Western blot (lane *c*) shows that both polypeptides cross reacted with the affinity-purified H1 antibodies. These results indicate that the H1 antibodies detect two polypeptides in squid optic lobe that differ in their relative molecular masses—one of which comigrates at the H2 region on gels. Fig. 11, lane *b*, is of the gel of the 19–20-*S* fraction, and one gel band is evident at the H2 region of the gel. However, within this area there was both bright orange and jet black staining, suggesting that H1 and H2 polypeptides were present but not resolved into two distinct bands. The corresponding Western blot (lane *d*) shows cross-reaction with the H1 antibodies. These data indicate that most of the H1 polypeptide sediments at 12–13 *S*, but there is a 19–20-*S* species also. Furthermore, the sedimentation of H2 at 19–20 *S* with the H1 polypeptide suggests that these polypeptides may represent heavy chains of a dynein-like molecule.

Negatively stained preparations of the 19–20-*S* fraction reveal double- and single-headed particles when a field of view is examined by transmission electron microscopy (Fig. 12). Fig. 13 shows several selected individual particles, and the two-headed particles (Fig. 13 *A*) exemplify the substructure of outer arm axonemal dyneins that sediment at 18–22 *S* (23, 26, 35, 43, 58, 82). Furthermore, the cytoplasmic dyneins, MAP 1C (76) and sea urchin egg dynein (30), also demonstrate this axonemal dynein morphology. Examination of the substructure of the squid double-headed particles reveals two individual globular heads that appear either pear shaped or spherical. These globular domains are connected by thin stems that contact each other and are joined at a common base. The single-headed particles (Fig. 13 *B*) appear either with or without tails and can be spherical or more elliptical in shape. Furthermore, the dimensions of the single-headed particles are comparable with those of the double-headed particles. These electron micrographs indicate that the protein purified at 19–20 *S* is a squid isoform of dynein.

Discussion

Purification of an Organelle Translocator

With the addition of MgATP to optic lobe microtubules, the H1 and H2 polypeptides were released to the resulting supernatant (Fig. 2) and further purified by gel filtration chromatography (Fig. 3 *A*). Furthermore, the column-purified protein demonstrated a soluble MgATPase activity and promoted the motility of salt-extracted vesicles and latex beads along microtubules (Figs. *5* and *6*). These results clearly indicated the presence of an ATP-dependent organelle translocator, and previous experiments (21) suggested that H1 and possibly H2 were polypeptides of this translocator complex. Both H1 and H2 polypeptides were associated with isolated axoplasmic vesicles that were observed to translocate on isolated microtubules (21, 22), and H1 bound [α^{32}P]8-azidoATP when H1 was in association with axoplasmic vesicles (21) or soluble as purified by gel filtration chromatography (Fig. 3 *B*). However, with the experimental conditions used, H2 was not observed to bind the radioactive photoaffinity analogue of ATP.

The affinity-purified antibodies to H1 localized the H1 antigen to vesicle-like particles in dissociated axoplasm (Fig. 8), and the punctate staining pattern of H1 demonstrated that in squid axoplasm H1 was a vesicle-associated polypeptide rather than a MAP that bound microtubules in a spatially periodic fashion. These immunofluorescence studies used a preparation of axoplasm that was diluted in a low ionic strength buffer and then dispersed by pipetting to yield a homogeneous preparation of single transport filaments. Therefore, this type of preparation allowed us to assess the local-

Figure 10. Sucrose density gradient analysis of H1/H2. The supernatant that results after extraction of microtubules with 10 mM MgATP was clarified, concentrated, and applied to 5–25% sucrose gradients. Each of the 18 fractions (1–18 top to bottom of the gradient) was analyzed for ATPase activity and by SDS-PAGE. *A* shows a silver-stained 4–10% acrylamide, 2–8 M urea gradient gel. *B* shows the absorbance at 280 nm (●) and the ATPase activity (△) expressed as nmol $^{32}P_i$/min per ml. Peaks of ATPase activity at 12–13 *S* (fractions *3–5*) and 19–20 *S* (fractions *10–12*) correspond to fractions containing high molecular mass polypeptides in *A*. Molecular mass markers are indicated to the left of *A*. *SS*, starting sample; *T*, tubulin subunits; *if*, ion front.

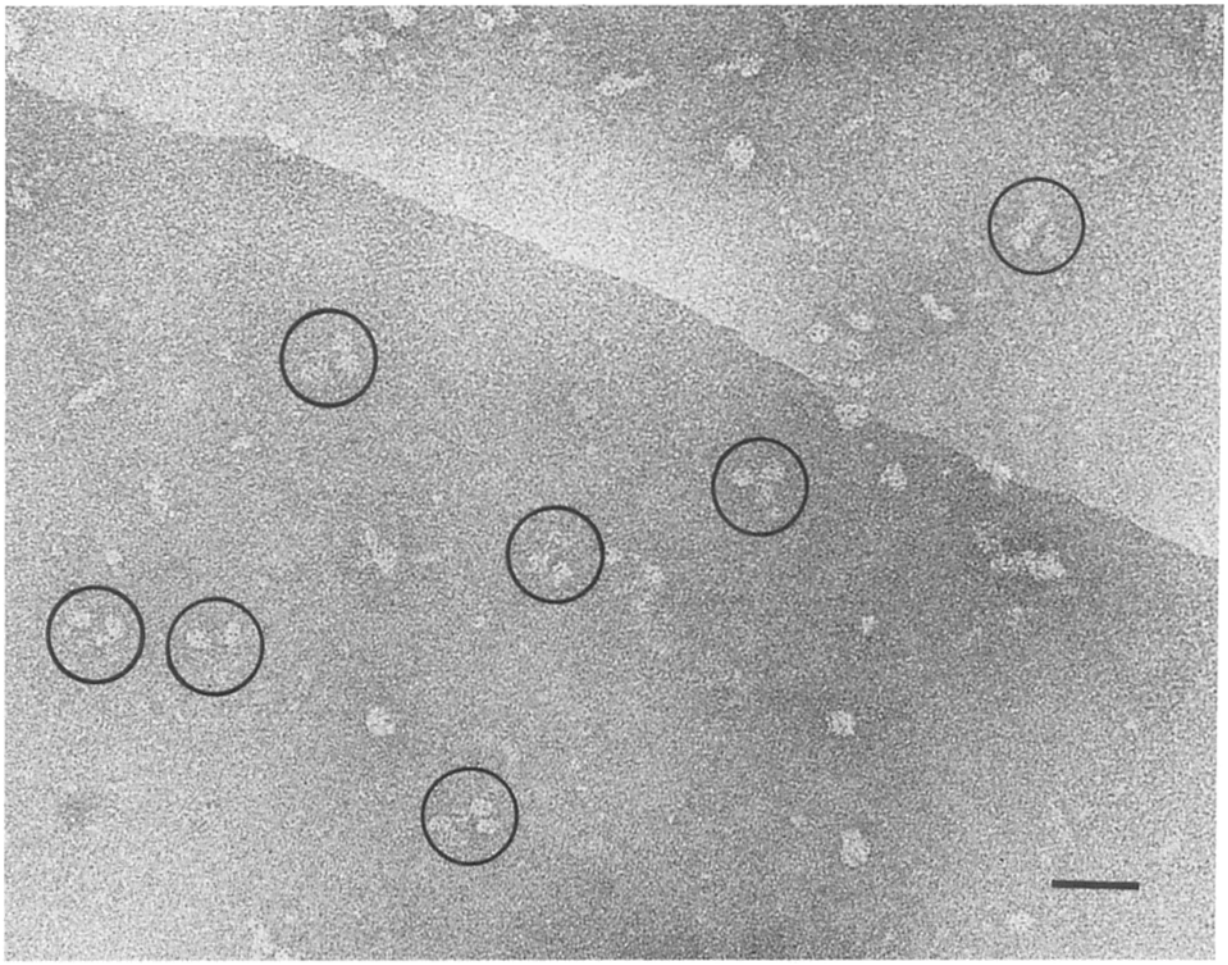

Figure 12. Negatively stained preparation of the 19–20-*S* sucrose gradient fraction. This low magnification view of the 19–20-*S* fraction shows the presence of two-headed (*circles*) and single-headed particles. Bar, 54 nm.

ization of the Hl antigen to vesicles, microtubules, or other particulate structures but could not give information about a soluble pool of Hl in axoplasm.

The Hl antibodies were also used in motility studies with dissociated axoplasm to determine the effect of the antibodies on vesicle movement. In such an approach, the Hl antibodies inhibited vesicle translocation bidirectionally in a concentration-dependent manner, yet various control preparations at the same concentration showed no detectable effect on vesicle motility (Table I). This result would be expected if both orthograde and retrograde vesicles carry motor molecules on their surface for both plus end–directed and minus end–directed movement—kinesin for plus end or orthograde movement, and the Hl/H2 complex for retrograde movement. According to this hypothesis, the direction of translocation would then be specified by the activation of one translocator and inactivation of the other, yet antibodies to one motor could inhibit both directions of movement—one specifically and one nonspecifically. However, the data cannot exclude the possibility that the Hl antibodies did bind Hl on the vesicle surface but sterically and therefore nonspecifically prevented interactions between the vesicle and microtubule that normally would be mediated by other mechanochemical enzymes.

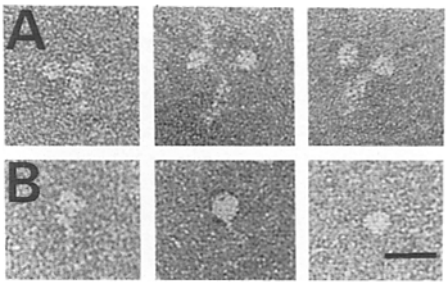

Figure 13. Representative two- and single-headed particles found in the 19–20-*S* fraction from sucrose gradients. The globular heads of both types of particles appear either pear shaped or spherical. Bar, 32 nm.

The observation that the gel filtration preparation of Hl/H2 promoted the translocation of both salt-extracted vesicles and latex beads indicated the presence of an organelle translocator (Figs. 5 and 6). The purification procedure used and the analysis of the motility suggested that the translocations observed were not mediated by trace amounts of kinesin that might have purified with the Hl and H2 polypeptides. First, GTP was included in the homogenization and microtubule isolation buffers; therefore, under these conditions kinesin would remain soluble and not copurify with microtubules and associated proteins (64, 72). The gels (Fig. 2) did not

show the presence of distinct polypeptides of ~110 kD nor did immunoblots of the optic lobe microtubules (from which H1 and H2 were purified) show cross-reaction when probed with rabbit polyclonal antibodies to the heavy chain of squid kinesin (data not shown). Second, the mean rates for both salt-extracted vesicles and latex beads at 0.9 μm/s are faster than the rate of 0.3–0.5 μm/s expected for squid kinesin (72). Although some translocations promoted by the gel filtration preparations were characterized by rates as low as 0.5 μm/s (Fig. 6), these translocations contained several pauses or hesitations, and the data represent the average speed of a vesicle or bead during the time of translocation. Lastly, microtubule gliding, a distinct characteristic of kinesin (64, 72, 73), was not promoted by the gel filtration protein that promoted the salt-extracted vesicle and bead motility.

Evaluation of the Translocator as a Squid Isoform of Dynein

Previously, we had shown that the H1 polypeptide cross reacted with a polyclonal antiserum to porcine brain MAP 2 (21), and Fig. 1 demonstrates the thermosolubility of H1. Do et al. (12) observed that this boiled preparation of H1 retained the ability to stimulate the assembly of chick brain tubulin and thus showed that H1 demonstrated some of the characteristics of a microtubule-associated polypeptide as originally defined (67, 68) and specifically of mammalian brain MAP 2 (16, 28, 36). However, when immunoblots containing porcine brain microtubules were probed with the H1 antibodies, the cross-reactions with MAP 2 were very weak—slightly above background (Fig. 7). The affinity-purified H1 antibodies were also used in double label immunofluorescence experiments, and Fig. 8 *B* shows that the H1 fluorescence pattern was punctate and corresponded to vesicle-like particles in the DIC micrograph of the preparation. The H1 fluorescence staining did not correspond to the smooth, linear pattern generated by fluorescent MAP 2 (60, 77). These results indicate that, in squid axoplasm, H1 was associated with vesicle-like particles rather than the axoplasmic microtubules in a spatially periodic fashion expected of a MAP 2–like polypeptide. Therefore, H1 may share one or more antigenic determinants with mammalian MAP 2 as suggested by the cross-reaction with the MAP 2 antiserum (21) and may have characteristics in common with mammalian MAP 2, but the results presented here indicate that H1 is not the squid analogue of vertebrate brain MAP 2.

The role of H2 in promoting the motility of vesicles and beads was not clear because H2 did not release to the supernatant stoichiometrically with H1 in the presence of 10 mM MgATP. In fact, when H1 and H2 were separated (Fig. 9), H2 sedimented with the microtubules even in the presence of MgATP. Furthermore, H2 was not observed to bind [α^{32}P]8-azidoATP (Fig. 3 *B* and reference 21, Fig. 2) as expected for a dynein heavy chain (9, 51, 54). However, in the presence of MgATP and vanadate, H2 was cleaved by UV irradiation to yield peptide fragments of 240 and 195 kD (Fig. 9), a distinctive characteristic of dynein. These results indicated that H2 was an ATP-binding polypeptide. Furthermore, the generation of the two vanadate-induced photocleavage peptides, each of ~200 kD, suggested that the ATP-binding site of H2 and its location within the polypeptide was similar to the ATP-binding site of axonemal and cytoplasmic dyneins (13, 19, 37, 40, 42, 47, 49, 52).

When the MgATP extracts from optic lobe microtubules were fractionated by sucrose density gradient ultracentrifugation, H1 and H2 sedimented together at 19–20 *S* (Figs. 10 and 11), and negatively stained preparations (Figs. 12 and 13) of the 19–20-*S* fraction revealed double-headed particles whose substructure was analogous to that of outer arm 18–22-*S* axonemal dyneins (23, 26, 35, 43, 58, 82) and cytoplasmic dyneins (30, 76). These results indicate that the vesicle and bead motility observed was promoted by a squid dynein-like protein. Furthermore, the results suggest that the double-headed particles are heterodimers containing one each of the H1 and H2 polypeptides. However, the sedimentation profile of the MgATP extract indicated that only a small proportion of the H1 and H2 polypeptides and associated ATPase activity sedimented at 19–20 *S* (Fig. 10). Fig. 9 shows that in the presence of MgATP most of the H2 sedimented with the microtubules in contrast to H1 which remained soluble. When the clarified MgATP extract was fractionated on sucrose gradients, most of the H1 and its associated ATPase activity sedimented at 12–13 *S*; and electron micrographs (data not shown) of the 12–13-*S* fraction reveal a number of single-headed particles. One characteristic of axonemal and sea urchin unfertilized egg dyneins is that the sedimentation of the dynein heavy chains and associated ATPase activity can be shifted from 18–20 *S* to 12–14 *S* by the presence of high or low salt or nonionic detergents such as Triton X-100 (14, 17, 18, 50, 52, 58, 69). Thus, the sedimentation of most of H1 at 12–13 *S* may represent a salt-dependent conformational change of the 19–20-*S* double-headed particle to a 12–13-*S* single-headed particle.

The sucrose gradient analysis (Fig. 10) and resulting immunoblots shown in Fig. 11 indicate that there are two molecular mass species of H1 in optic lobe, but only the lower relative molecular mass species sediments at 19–20 *S*. The role of the higher relative molecular mass species is not known at this time, but it may represent a precursor form that requires some form of modification for activity. Furthermore, because optic lobe is characterized by large nerve endings, cell bodies, dendrites as well as glial and granule cells but not long segments of axons (10, 25), the two molecular mass forms of H1 may be characteristic of these neuronal compartments and cell types but not characteristic of axonal compartments. These questions can be resolved with further experimentation using 19–20-*S* fractions from axoplasm.

The data presented indicate that the motility promoted by the gel filtration preparation of H1/H2 is due to a squid isoform of dynein. Furthermore, the H1 and H2 polypeptides sediment at 19–20 *S*, and preparations negatively stained for electron microscopy reveal a double-headed dynein-like particle at 19–20 *S*. However, the results presented here do not conclusively show that H1 and H2 are the polypeptides that correspond to the heads of the double-headed particles detected by electron microscopy and therefore are the dynein heavy chains. However, if one assumes that H1 and H2 are the heavy chain polypeptides of the double-headed dynein, then the results from the [α^{32}P]8-azidoATP-binding and UV vanadate-sensitive cleavage experiments suggest that the nucleotide-binding sites of H1 and H2 are different. H1 was observed to bind [α^{32}P]8-azidoATP, yet H2 did not with the experimental conditions used (Fig. 3 and reference 21, Fig. 2). Furthermore, H2 was cleaved by ADP·vanadate·UV but H1 cleavage peptides were not generated (Fig. 9). A model that accounts for these observations follows: when the high speed

optic lobe supernatant is prepared, squid dynein is present as the double-headed particle and as single-headed particles of H1 or H2. During taxol assembly of microtubules, both the double- and single-headed particles would sediment with the microtubules and, in the presence of MgATP, both types of particles would be released from the microtubules to the supernatant. However, the gels (Fig. 9) indicate that most of the H2 sediments with the microtubules, yet the H1 remains soluble. Therefore, when the MgATP extract enriched in H1 is fractionated by sucrose density gradient centrifugation, the single-headed H1 would sediment at 12–13 *S* and the double-headed particle (H1/H2 [1:1]) would sediment at 19–20 *S*. This behavior predicts that the rate of release of ADP from H1 would be faster than the rate of release of ADP from H2, a fact which would also explain our inability to detect the binding of [α^{32}P]8-azidoATP by H2.

The [α^{32}P]8-azidoATP binding and the UV cleavage results suggest that the nucleotide-binding domains of the squid dynein heavy chain polypeptides are somewhat different from those of the axonemal dyneins. For example, Pfister et al. (51) showed that both the α and β heavy chains of *Chlamydomonas* 18-*S* dynein bind [α^{32}P]8-azidoATP. Pratt (54) demonstrated that in the case of sea urchin flagellar and unfertilized egg dyneins the two heavy chains (A and B) bound [α^{32}P]8-azidoATP. Furthermore, each of the three heavy chains of outer arm ciliary dynein from *Tetrahymena* was labeled by [2-^{3}H]8-azidoATP and to approximately the same extent (9). The observation that H1 bound [α^{32}P]8-azidoATP yet H2 did not suggests that at the time of labeling with the photoaffinity analogue H2 already had nucleotide bound at its active site. Thus, because of the low efficiency of labeling by the photoaffinity azidoATP analogues (53), we were not able to detect [α^{32}P]8-azidoATP labeling by H2.

UV vanadate-specific cleavage of H1 was not detected (Fig. 9, lanes *q* and *r*), suggesting that the nucleotide-binding sites of H1 and H2 are different. For the axonemal dyneins and some of the cytoplasmic dyneins recently characterized, significant photocleavage of the heavy chains occurs within minutes and almost complete cleavage is obtained by 30–60 min (19, 37, 40, 42, 47, 52). In the case of the squid protein as well as MAP 1C, significant amounts of the heavy chain remained intact after 120 min of irradiation; and for MAP 1C, substantial amounts remained after irradiation for 5 h (Fig. 12 of reference 49). Although these data are consistent with a difference in nucleotide-binding sites of the heavy chains (H1 and H2) of squid dynein as well as another cytoplasmic dynein, MAP 1C, it is possible that the results observed reflect heterogeneity in the activity of the purified protein. More quantitative approaches that examine these ATPases at their active sites will be required to determine if there is truly a difference in the nucleotide-binding sites of these dynein heavy chains.

The results presented characterize a squid isoform of dynein. The H1 and H2 polypeptides are high molecular mass MAPs (relative molecular mass of ~435 kD) that interact with microtubules in an ATP-sensitive manner. The soluble protein purified by gel filtration demonstrates MgATPase activity and promotes the translocation of both latex beads and salt-extracted vesicles along isolated microtubules at a rate of ~0.9 μm/s. H1 and H2 polypeptides and associated ATPase activity sediment at 19–20 *S*, electron microscopy reveals a double-headed dynein-like particle in this fraction, the H1 polypeptide binds [α^{32}P]8-azidoATP, and the H2 polypeptide demonstrates vanadate-induced UV photocleavage. Lastly, the immunofluorescence data localize the H1 polypeptide to vesicle-like particles in squid axoplasm which indicate that this neuronal dynein promotes membranous organelle motility during fast axoplasmic transport. Thus, this squid dynein isoform composed of at least two different high molecular mass polypeptides appears to be a member of the family of nonaxonemal dyneins that have been recently characterized.

We thank Dr. Lester I. Binder (University of Alabama, Birmingham, Alabama) for monoclonal antibodies to β-tubulin, Drs. Karl Fath and Raymond J. Lasek (Case Western Reserve University School of Medicine, Cleveland, OH) for myosin preimmune and antisera, Dr. Margaret A. Titus (Stanford University School of Medicine, Stanford, CA) for rabbit skeletal myosin, and Dr. Matthew Suffness (National Cancer Institute, Bethesda, MD) for taxol. S. P. Gilbert gratefully acknowledges Drs. Tamie J. Chilcote, Erika L. F. Holzbaur, Isaac Wong (Pennsylvania State University, University Park, PA) for sharing their expertise of the ATPase assays and computer programs for data analysis and Dr. Sid Marchese-Ragona for his guidance and assistance with the electron microscopy. S. P. Gilbert is most appreciative to Dr. Kenneth A. Johnson (Pennsylvania State University) for giving her the time as well as his support both at Pennsylvania State University and at the Marine Biological Laboratory (Woods Hole, MA) during her postdoctoral training to complete these studies.

This research was supported by grants to R. D. Sloboda (BNS 85-03597 from the National Science Foundation, the Muscular Dystrophy Association, and the Biomedical Research Science Fund administered by Dartmouth College), K. A. Johnson (GM26726 from the National Institutes of Health), and S. P. Gilbert (postdoctoral fellowship from the Muscular Dystrophy Association and the H. Burr Steinbach Fellowship from the Marine Biological Laboratory).

Received for publication 28 December 1987 and in revised form 12 July 1989.

References

1. Allen, R. D., and N. S. Allen. 1983. Video-enhanced microscopy with a computer frame memory. *J. Microsc. (Oxf.).* 129:3–17.
2. Allen, R. D., D. G. Weiss, J. H. Hayden, D. T. Brown, H. Fujiwake, and M. Simpson. 1985. Gliding movement of and bidirectional transport along single native microtubules from squid axoplasm: evidence for an active role of microtubules in cytoplasmic transport. *J. Cell Biol.* 100:1736–1752.
3. Bell, C. W., C. Fraser, W. S. Sale, W. -J. Y. Tang, and I. R. Gibbons. 1982. Preparation and purification of dynein. *Methods Cell Biol.* 24:373–297.
4. Blake, M. S., K. H. Johnston, G. J. Russell-Jones, and E. C. Gotschlich. 1984. A rapid, sensitive method for detection of alkaline phosphatase–conjugated anti-antibody on Western blots. *Anal. Biochem.* 136: 175–179.
5. Borisy, G. G., J. B. Olmsted, J. M. Marcum, and C. Allen. 1974. Microtubule assembly in vitro. *Fed. Proc.* 33:167–174.
6. Bradford, M. M. 1976. A rapid and sensitive method for the quantitation of microgram quantities of protein utilizing the principle of protein-dye binding. *Anal. Biochem.* 72:248–254.
7. Brady, S. T., 1985. A novel brain ATPase with properties expected for the fast axonal transport motor. *Nature (Lond.).* 317:73–75.
8. Burton, P. R., and J. L. Paige. 1981. Polarity of axoplasmic microtubules in the olfactory nerve of the frog. *Proc. Natl. Acad. Sci. USA.* 78:3269–3273.
9. Chilcote, T. J. 1988. The Dynein ATPase Pathway: ATP Analogs and Regulation by Phosphorylation. Ph.D. thesis. The Pennsylvania State University, University Park, PA. 174 pp.
10. Cohen, A. I. 1973. An ultrastructural analysis of the photoreceptors of the squid and their synaptic connections. III. Photoreceptor terminations in the optic lobes. *J. Comp. Neurol.* 147:399–426.
11. Dentler, W. L., S. Granett, and J. L. Rosenbaum. 1975. Ultrastructural localization of the high molecular weight proteins associated with in vitro–assembled brain microtubules. *J. Cell Biol.* 65:237–241.
12. Do, C. V., E. B. Sears, S. P. Gilbert, and R. D. Sloboda. 1988. Vesikin, a vesicle associated ATPase from squid axoplasm and optic lobe, has characteristics in common with vertebrate Brain MAP 1 and MAP 2. *Cell*

Motil. Cytoskeleton. 10:246–254.
13. Euteneuer, U., M. P. Koonce, K. K. Pfister, and M. Schliwa. 1988. An ATPase with properties expected for the organelle motor of the giant amoeba, *Reticulomyxa. Nature (Lond.).* 332:176–178.
14. Evans, J. A., and I. R. Gibbons. 1986. Activation of dynein 1 adenosine triphosphatase by organic solvents and by Triton X-100. *J. Biol. Chem.* 261:14044–14048.
15. Fairbanks, G., T. L. Steck, and D. F. H. Wallach. 1971. Electrophoretic analysis of the major polypeptides of the human erythrocyte membrane. *Biochemistry.* 10:2606–2617.
16. Fellous, A., J. Francon, A. -M. Lennon, and J. Nunez. 1977. Microtubule assembly *in vitro*: purification of assembly-promoting factors. *Eur. J. Biochem.* 78:167–174.
17. Foltz, K. R., and D. J. Asai. 1988. Ionic strength–dependent isoforms of sea urchin egg dynein. *J. Biol. Chem.* 263:2878–2883.
18. Gibbons, I. R., and E. Fronk. 1979. A latent adenosine triphosphatase form of dynein 1 from sea urchin sperm flagella. *J. Biol. Chem.* 254:187–196.
19. Gibbons, I. R., A. Lee-Eiford, G. Mocz, C. A. Phillipson, W. -J. Y. Tang, and B. H. Gibbons. 1987. Photosensitized cleavage of dynein heavy chains: cleavage at the "V1 site" by irradiation at 365 nm in the presence of ATP and vanadate. *J. Biol. Chem.* 262:2780–2786.
20. Gilbert, S. P., and R. D. Sloboda. 1984. Bidirectional transport of fluorescently labeled vesicles introduced into extruded axoplasm of squid *Loligo pealei. J. Cell Biol.* 99:445–452.
21. Gilbert, S. P., and R. D. Sloboda. 1986. Identification of a MAP 2-like ATP-binding protein associated with axoplasmic vesicles that translocate on isolated microtubules. *J. Cell Biol.* 103:947–956.
22. Gilbert, S. P., R. D. Allen, and R. D. Sloboda. 1985. Translocation of vesicles from squid axoplasm on flagellar microtubules. *Nature (Lond.).* 315:245–248.
23. Goodenough, U., and J. Heuser. 1984. Structural comparison of purified dynein proteins with *in situ* dynein arms. *J. Mol. Biol.* 180:1083–1118.
24. Grafstein, B., and D. S. Forman. 1980. Intracellular transport in neurons. *Physiol. Rev.* 60:1167–1283.
25. Haghighat, N., R. S. Cohen, and G. D. Pappas. 1984. Fine structure of squid (*Loligo pealei*) optic lobe synapses. *Neuroscience.* 13:527–546.
26. Hastie, A. T., S. P. Marchese-Ragona, K. A. Johnson, and J. S. Wall. Structure and mass of mammalian respiratory ciliary outer arm 19S dynein. *Cell Motil. Cytoskeleton.* 11:157–166.
27. Heidemann, S. R., J. M. Landers, and M. A. Hamborg. 1981. Polarity orientation of axonal microtubules. *J. Cell Biol.* 91:661–665.
28. Herzog, W., and K. Weber. 1978. Fractionation of brain microtubule-associated proteins: isolation of two different proteins which stimulate tubulin polymerization *in vitro. Eur. J. Biochem.* 92:1–8.
29. Hirokawa, N. 1986. 270K microtubule-associated protein cross-reacting with anti-MAP2 IgG in the crayfish peripheral nerve axon. *J. Cell Biol.* 103:33–39.
30. Hisanaga, S., and N. Hirokawa. 1987. Substructure of sea urchin egg cytoplasmic dynein. *J. Mol. Biol.* 195:919–927.
31. Hollenbeck, P. J., and K. Chapman. 1986. A novel microtubule-associated protein from mammalian nerve shows ATP-sensitive binding to microtubules. *J. Cell Biol.* 103:1539–1545.
32. Inoué, S. 1981. Video image processing greatly enhances contrast, quality, and speed in polarization-based microscopy. *J. Cell Biol.* 89:346–356.
33. Johnson, G. D., and G. M. de C. Nogueira Araujo. 1981. A simple method of reducing the fading of immunofluorescence during microscopy. *J. Immunol. Methods.* 43:349–350.
34. Johnson, K. A. 1983. The pathway of ATP hydrolysis by dynein: kinetics of a presteady state phosphate burst. *J. Biol. Chem.* 258:13825–13832.
35. Johnson, K. A., and J. S. Wall. 1983. Structure and molecular weight of the dynein ATPase. *J. Cell Biol.* 96:669–678.
36. Kim, H., L. I. Binder, and J. L. Rosenbaum. 1979. The periodic association of MAP_2 with brain microtubules in vitro. *J. Cell Biol.* 80:266–276.
37. King, S. M., and G. B. Witman. 1987. Structure of the α and β heavy chains of the outer arm dynein from *Chlamydomonas* flagella: masses of chains and sites of ultraviolet-induced vanadate-dependent cleavage. *J. Biol. Chem.* 262:17596–17604.
38. Laemmli, U. K. 1970. Cleavage of structural proteins during the assembly of the head of bacteriophage T4. *Nature (Lond.).* 227:680–685.
39. Lasek, R. J., and S. T. Brady. 1985. Attachment of transported vesicles to microtubules in axoplasm is facilitated by AMP-PNP. *Nature (Lond.).* 316:645–647.
40. Lee-Eiford, A., R. A. Ow, and I. R. Gibbons. 1986. Specific cleavage of dynein heavy chains by ultraviolet irradiation in the presence of ATP and vanadate. *J. Biol. Chem.* 261:2337–2342.
41. Lowry, O. H., N. J. Rosebrough, A. L. Farr, and R. J. Randall. 1951. Protein measurement with the folin phenol reagent. *J. Biol. Chem.* 193:265–275.
42. Lye, R. J., M. E. Porter, J. M. Scholey, and J. R. McIntosh. 1987. Identification of a microtubule-based cytoplasmic motor in the nematode *C. elegans. Cell.* 51:309–318.
43. Marchese-Ragona, S. P., C. Gagnon, D. White, M. Belles-Isles, and K. A. Johnson. 1987. Structure and mass analysis of 12S and 19S dynein obtained from bull sperm flagella. *Cell Motil.* 8:368–374.
44. Martin, R. G., and B. N. Ames. 1961. A method for determining the sedimentation behavior of enzymes: application to protein mixtures. *J. Biol. Chem.* 236:1372–1379.
45. Morrissey, J. H. 1982. Silver stain for proteins in polyacrylamide gels: a modified procedure with enhanced uniform sensitivity. *Anal. Biochem.* 117:307–310.
46. Murphy, D. B., and G. G. Borisy. 1975. Association of high-molecular-weight proteins with microtubules and their role in microtubule assembly *in vitro. Proc. Natl. Acad. Sci. USA.* 72:2696–2700.
47. Neely, M. D., and K. Boekelheide. 1988. Sertoli cell processes have axoplasmic features: an ordered microtubule distribution and an abundant high molecular weight microtubule-associated protein (cytoplasmic dynein). *J. Cell Biol.* 107:1767–1776.
48. Paschal, B. M., and R. B. Vallee. 1987. Retrograde transport by the microtubule-associated protein MAP 1C. *Nature (Lond.).* 330:181–183.
49. Paschal, B. M., H. S. Shpetner, and R. B. Vallee. 1987. MAP 1C is a microtubule-activated ATPase which translocates microtubules in vitro and has dynein-like properties. *J. Cell Biol.* 105:1273–1282.
50. Pfister, K. K., and G. B. Witman. 1984. Subfractionation of *Chlamydomonas* 18 S dynein into two unique subunits containing ATPase activity. *J. Biol. Chem.* 259:12072–12080.
51. Pfister, K. K., B. E. Haley, and G. B. Witman. 1985. Labeling of *Chlamydomonas* 18 S dynein polypeptides by 8-azidoadenosine 5′-triphosphate, a photoaffinity analog of ATP. *J. Biol. Chem.* 260:12844–12850.
52. Porter, M. E., P. M. Grissom, J. M. Scholey, E. D. Salmon, and J. R. McIntosh. 1988. Dynein isoforms in sea urchin eggs. *J. Biol. Chem.* 263:6759–6771.
53. Potter, R. L., and B. E. Haley. 1983. Photoaffinity labeling of nucleotide binding sites with 8-azidopurine analogs: techniques and applications. *Methods Enzymol.* 91:613–633.
54. Pratt, M. M. 1986. Homology of egg and flagellar dynein: comparison of ATP-binding sites and primary structure. *J. Biol. Chem.* 261:956–964.
55. Pratt, M. M. 1986. Stable complexes of axoplasmic vesicles and microtubules: protein composition and ATPase activity. *J. Cell Biol.* 103:957–968.
56. Pratt, M. M., S. Hisanaga, and D. A. Begg. 1984. An improved purification method for cytoplasmic dynein. *J. Cell. Biochem.* 26:19–33.
57. Rebhun, L. I. 1972. Polarized intracellular particle transport: saltatory movements and cytoplasmic streaming. *Int. Rev. Cytol.* 32:93–137.
58. Sale, W. S., U. W. Goodenough, and J. E. Heuser. 1985. The substructure of isolated and in situ outer dynein arms of sea urchin sperm flagella. *J. Cell Biol.* 101:1400–1412.
59. Schacterle, G. R., and R. L. Pollack. 1973. A simplified method for the quantitative assay of small amounts of protein in biologic material. *Anal. Biochem.* 51:654–655.
60. Scherson, T., T. E. Kreis, J. Schlessinger, U. Z. Littauer, G. G. Borisy, and B. Geiger. 1984. Dynamic interactions of fluorescently labeled microtubule-associated proteins in living cells. *J. Cell Biol.* 99:425–434.
61. Schliwa, M. 1984. Mechanisms of intracellular organelle transport. *Cell Muscle Motil.* 5:1–82.
62. Schnapp, B. J., R. D. Vale, M. P. Sheetz, and T. S. Reese. 1985. Single microtubules from squid axoplasm support bidirectional movement of organelles. *Cell.* 40:455–462.
63. Scholey, J. M., B. Neighbors, J. R. McIntosh, and E. D. Salmon. 1984. Isolation of microtubules and a dynein-like MgATPase from unfertilized sea urchin eggs. *J. Biol. Chem.* 259:6516–6525.
64. Scholey, J. M., M. E. Porter, P. M. Grissom, and J. R. McIntosh. 1985. Identification of kinesin in sea urchin eggs, and evidence for its localization in the mitotic spindle. *Nature (Lond.).* 318:483–486.
65. Shelanski, M. L., F. Gaskin, and C. R. Cantor. 1973. Microtubule assembly in the absence of added nucleotides. *Proc. Natl. Acad. Sci. USA.* 70:765–768.
66. Sloboda, R. D., and S. P. Gilbert. 1989. Microtubule associated proteins (MAPs) and microtubule dependent intracellular particle motility. *In* Cell Movement: Kinesin, Dynein, and Microtubule Dynamics. Vol. 2. F. D. Warner and J. R. McIntosh, editors. Alan R. Liss Inc., New York. 223–232.
67. Sloboda, R. D., and J. L. Rosenbaum. 1979. Decoration and stabilization of intact, smooth-walled microtubules with microtubule-associated proteins. *Biochemistry.* 18:48–55.
68. Sloboda, R. D., S. A. Rudolph, J. L. Rosenbaum, and P. Greengard. 1975. Cyclic AMP–dependent endogenous phosphorylation of a microtubule-associated protein. *Proc. Natl. Acad. Sci. USA.* 72:177–181.
69. Tang, W. -J. Y., C. W. Bell, W. S. Sale, and I. R. Gibbons. 1982. Structure of the dynein-1 outer arm in sea urchin sperm flagella. I. Analysis by separation of subunits. *J. Biol. Chem.* 257:508–515.
70. Towbin, H., T. Staehelin, and J. Gordon. 1979. Electrophoretic transfer of proteins from polyacrylamide gels to nitrocellulose sheets: procedure and some applications. *Proc. Natl. Acad. Sci. USA.* 76:4350–4354.
71. Vale, R. D. 1987. Intracellular transport using microtubule-based motors. *Annu. Rev. Cell Biol.* 3:347–378.
72. Vale, R. D., T. S. Reese, and M. P. Sheetz. 1985. Identification of a novel force-generating protein, kinesin, involved in microtubule-based motility. *Cell.* 42:39–50.

73. Vale, R. D., B. J. Schnapp, T. Mitchison, E. Steuer, T. S. Reese, and M. P. Sheetz. 1985. Different axoplasmic proteins generate movement in opposite directions along microtubules in vitro. *Cell.* 43:623–632.
74. Vale, R. D., B. J. Schnapp, T. S. Reese, M. P. Sheetz. 1985. Movement of organelles along filaments dissociated from the axoplasm of the squid giant axon. *Cell.* 40:449–454.
75. Valentine, R. C., B. M. Shapiro, and E. R. Stadtman. 1968. Regulation of glutamine synthetase. XII. Electron microscopy of the enzyme from *Escherichia coli. Biochemistry.* 7:2143–2152.
76. Vallee, R. B., J. S. Wall, B. M. Paschal, and H. S. Shpetner. 1988. Microtubule-associated protein 1C from brain is a two-headed cytosolic dynein. *Nature (Lond.).* 332:561–563.
77. Vandenbunder, B., and G. G. Borisy. 1986. Decoration of microtubules by fluorescently labeled microtubule-associated protein 2 (MAP2) does not interfere with their spatial organization and progress through mitosis in living fibroblasts. *Cell Motil. Cytoskeleton.* 6:570–579.
78. Vogel, A. I. 1961. A Textbook of Quantitative Inorganic Analysis. John Wiley & Sons Inc., New York. 790–791.
79. Warner, F. D., and J. R. McIntosh. 1989. Cell Movement: Kinesin, Dynein, and Microtubule Dynamics. Volume 2. Alan R. Liss Inc., New York. 487 pp.
80. Warner, F. D., P. Satir, and Ian R. Gibbons. 1989. Cell Movement: The Dynein ATPases. Vol. 1. Alan R. Liss Inc., New York. 337 pp.
81. Warren, R. H. 1984. Axonal microtubules of crayfish and spiny lobster nerve cords are decorated with a heat-stable protein of high molecular weight. *J. Cell Sci.* 71:1–15.
82. Witman, G. B., K. A. Johnson, K. K. Pfister, and J. S. Wall. 1983. Fine structure and molecular weight of the outer arm dyneins of *Chlamydomonas. J. Submicrosc. Cytol.* 15:193–197.